# The simulation of low Mach flows: from the AUSM-IT flux scheme to ATCBC boundary conditions

Pascal Bruel

# The simulation of low Mach flows: from the AUSM-IT flux scheme to ATCBC boundary conditions


Pascal Bruel

CNRS

Inria Project-Team Cagire

(www.inria.fr/en/teams/cagire)

Lab of Mathematics and their Applications

Pau University – France


Universidad Nacional de Córdoba - Argentina

30 March 2017

## Presentation Layout

1. The industrial context

2. A low Mach flux for low order FV method

3. Prescribing unsteady subsonic inlet boundary conditions

# Industrial context: combustion chamber cooling


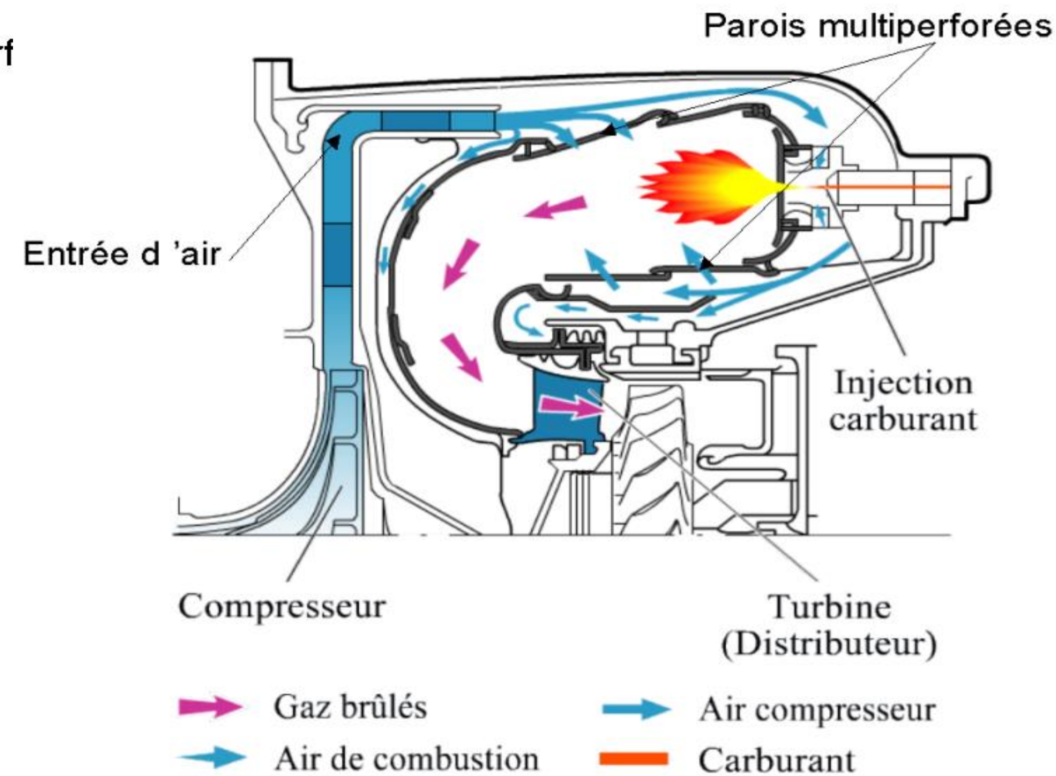

# Industrial context: combustion chamber cooling

## Different wall cooling approaches

| | |
|---|---|
| Film cooling<br>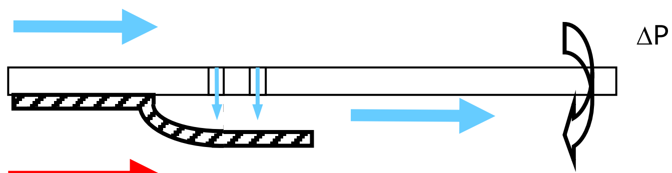 | ☺ Easy to manufacture<br>☹ Short protection length |
| Double wall<br>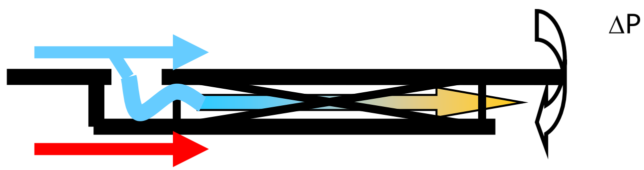 | ☺ No local perturbation of the flow<br>☹ Modest cooling efficiency |
| Multiperforations<br>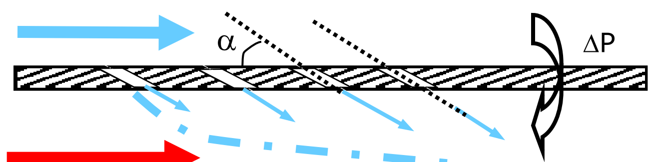 | ☺ High cooling efficiency over the perforated plate<br>☹ Important flow rate (~30% of total air supplied to the chamber) |

Hot gases (≈ 2200K) Cooling air (≈ 600K)

# Industrial context: combustion chamber cooling

- ➔ **Combustion chamber cooling through multiperforated surfaces « effusion cooling »**
- ➔ **Canonica**

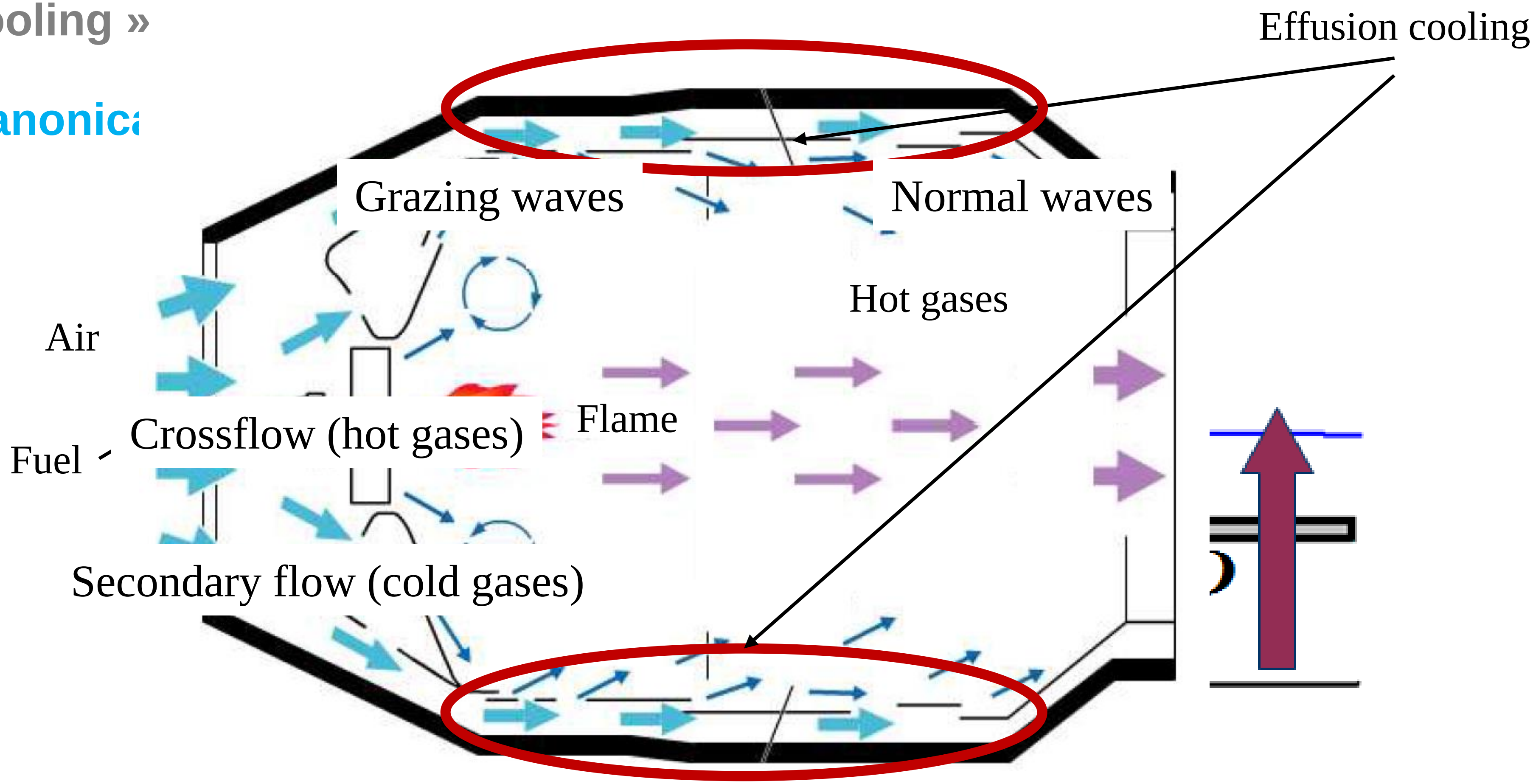

# Industrial context: combustion chamber cooling

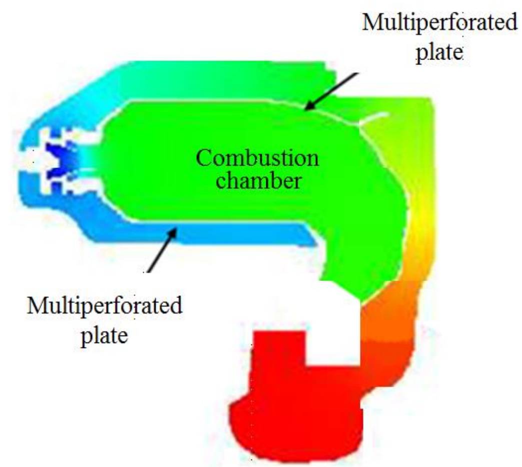


## ➔ Acoustic sources

- Combustion noise (up to 80dB)
- Thermoacoustic instabilities (up to 140dB)
- Mechanical vibrations
- …

## ➔ Acoustic modes:

- Longitudinal
- Radial
- Azimuthal

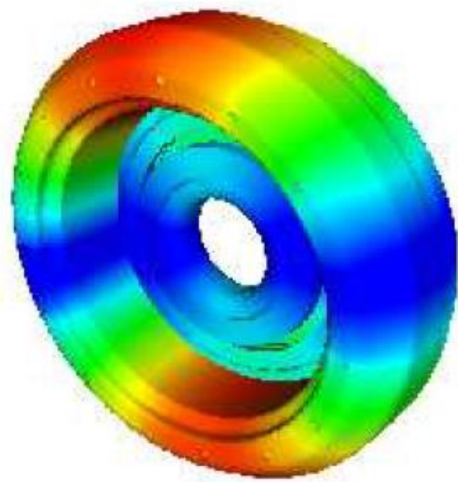

## ➔ Wave types:

- Steady (all modes)
- Propagating (azimuthal modes essentially)

# Illustration of a turbulent reacting flow with turbulence and deterministic motion obtained on the ORACLES test facility (Nguyen et al., 2009)

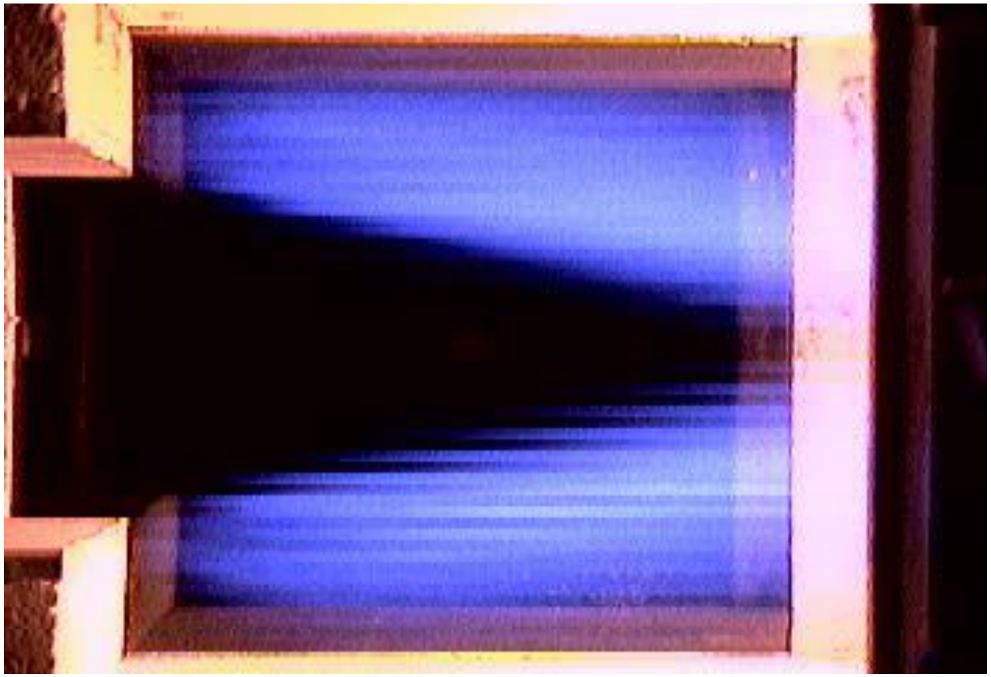

Exposure time: 1/50 s

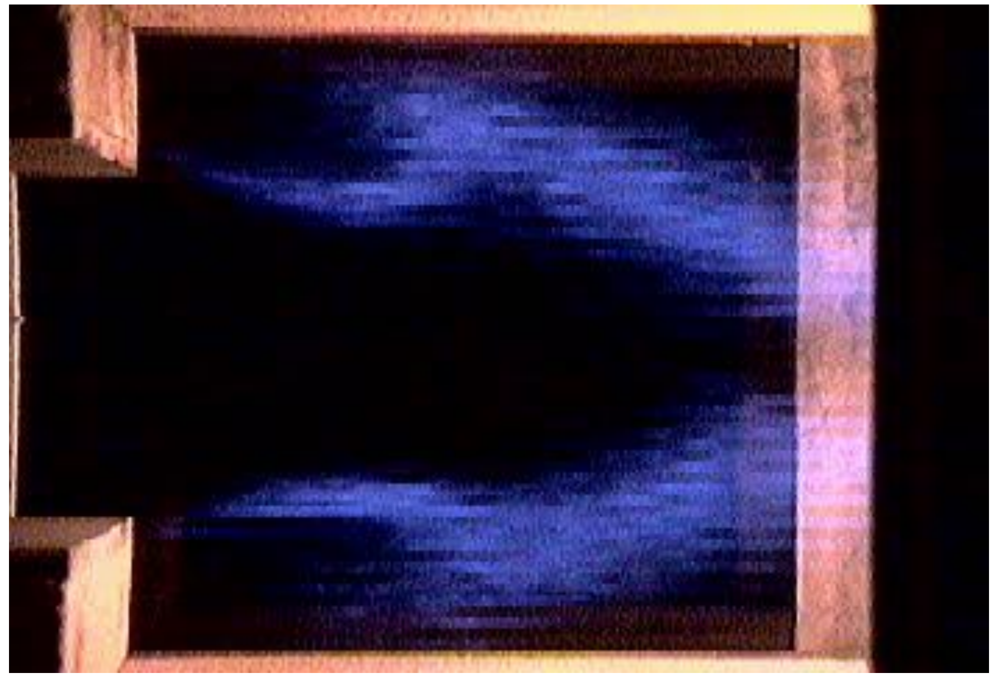

Exposure time: 1/2000 s

# Low Mach flows: a better insight about the major players with an asymptotic expansion of the governing equations

Using a single space scale and two time scales $t_{conv}$ and $t_{ac} = t_{conv} / \hat{M}$,

any field variable, for instance for the pressure, is expanded as:

$$p(\boldsymbol{x},t;\hat{M}) = p^{(0)}(x,t_{conv},t_{ac}) + \hat{M}\; p^{(1)}(x,t_{conv},t_{ac}) + \hat{M}^2 p^{(2)}(x,t_{conv},t_{ac}) + O(\hat{M}^3)$$

The time derivative at constant $x$ and $\hat{M}$ yields (chain rule):

$$\left.\frac{\partial}{\partial t}\right|_{\mathbf{x},\hat{M}} = \frac{\partial}{\partial t_{conv}}\frac{\partial t_{conv}}{\partial t} + \frac{\partial}{\partial t_{ac}}\frac{\partial t_{ac}}{\partial t} = \frac{\partial}{\partial t} + \frac{1}{\hat{M}}\frac{\partial}{\partial t_{ac}}$$

From now, whenever relevant, we shall retain the simpler notation: $t_{conv} \equiv t$ and $t_{ac} \equiv \tau$

# Low Mach flows: a better insight about the major players with an asymptotic expansion of the governing equations

If one proceeds similarly as before, the zeroth, first and second order equations yields:

Continuity

$$\frac{\partial \rho^{(0)}}{\partial \tau} = 0 \Rightarrow \rho^{(0)} = \rho^{(0)}(\boldsymbol{x}, t)$$

$$\frac{\partial \rho^{(1)}}{\partial \tau} + \frac{\partial \rho^{(0)}}{\partial t} + \nabla.(\rho \boldsymbol{u})^{(0)} = 0$$

$$\frac{\partial \rho^{(2)}}{\partial \tau} + \frac{\partial \rho^{(1)}}{\partial t} + \nabla.(\rho \boldsymbol{u})^{(1)} = 0$$

Momentum

$$\nabla p^{(0)} = 0 \Rightarrow p^{(0)} = p^{(0)}(t)$$

$$\frac{\partial (\rho \boldsymbol{u})^{(0)}}{\partial \tau} = -\nabla p^{(1)} \Rightarrow \frac{\partial \boldsymbol{u}^{(0)}}{\partial \tau} = -\frac{1}{\rho^{(0)}} \nabla p^{(1)}$$

$$\frac{\partial (\rho \boldsymbol{u})^{(1)}}{\partial \tau} + \frac{\partial (\rho \boldsymbol{u})^{(0)}}{\partial t} + \nabla.(\rho \boldsymbol{u} \otimes \boldsymbol{u})^{(0)} = -\nabla p^{(2)} + \frac{1}{\mathrm{Re}} \nabla.\boldsymbol{\tau}^{(0)}$$

# Low Mach flows: a better insight about the major players with an asymptotic expansion of the governing equations

## Energy equation

$$\frac{\partial(\rho E)^{(0)}}{\partial \tau} = 0$$

$$\frac{\partial(\rho E)^{(1)}}{\partial \tau} + \frac{\partial(\rho E)^{(0)}}{\partial t} + \nabla.(\rho \boldsymbol{u} H)^{(0)} = \frac{\gamma}{\gamma - 1}\frac{1}{\Pr \mathrm{Re}}\nabla.(\lambda \nabla T)^{(0)} + (\rho q)^{(0)}$$

$$\frac{\partial(\rho E)^{(2)}}{\partial \tau} + \frac{\partial(\rho E)^{(1)}}{\partial t} + \nabla.(\rho \boldsymbol{u} H)^{(1)} = \frac{\gamma}{\gamma - 1}\frac{1}{\Pr \mathrm{Re}}\nabla.(\lambda \nabla T)^{(1)} + (\rho q)^{(1)}$$

## State equations

$$\rho^{(0)}(t,x)T^{(0)}(t,x) = p^{(0)}(t)$$

$$p^{(0)}(t) = (\gamma - 1)(\rho E)^{(0)}(t)$$

# Low Mach flows: a better insight about the major players with an asymptotic expansion of the governing equations

The first order energy equation can be also expressed as:

$$\frac{\partial p^{(1)}}{\partial \tau} + \gamma p^{(0)} \nabla.(\boldsymbol{u})^{(0)} = \gamma \frac{1}{\Pr \mathrm{Re}} \nabla.(\lambda \nabla T)^{(0)} + (\gamma - 1)(\rho q)^{(0)} - \frac{dp^{(0)}}{dt}$$

Differentiating the above equation with respect to $\tau$ and substracting $\gamma p^{(0)}$ times the divergence of the first order momentum equation yields:

$$\frac{\partial^2 p^{(1)}}{\partial \tau^2} - \nabla.(c^{(0)^2} \nabla p^{(1)})^{(0)} = (\gamma - 1) \frac{\partial (\rho q)^{(0)}}{\partial \tau} \text{ with } c^{(0)^2} = \gamma \frac{p^{(0)}(t)}{\rho^{(0)}(\boldsymbol{x}, t)}$$

This is a wave equation and its source is the change **over acoustic time** of the **leading order of the heat release rate.**

# Effusion cooling: The related canonical flow is the jet in cross flow (JICF)

- Examples of experiments:
  - Frick and Roshko (1994), Kelso et al. (1996), Smith and Mungal (1998), Gustafsson (2001), M'Closkey et al. (2001), Most (2007), Michel (2010), Ali (2010),….

Freely adapted from Frick and Roshko (1994)

Flow structure:

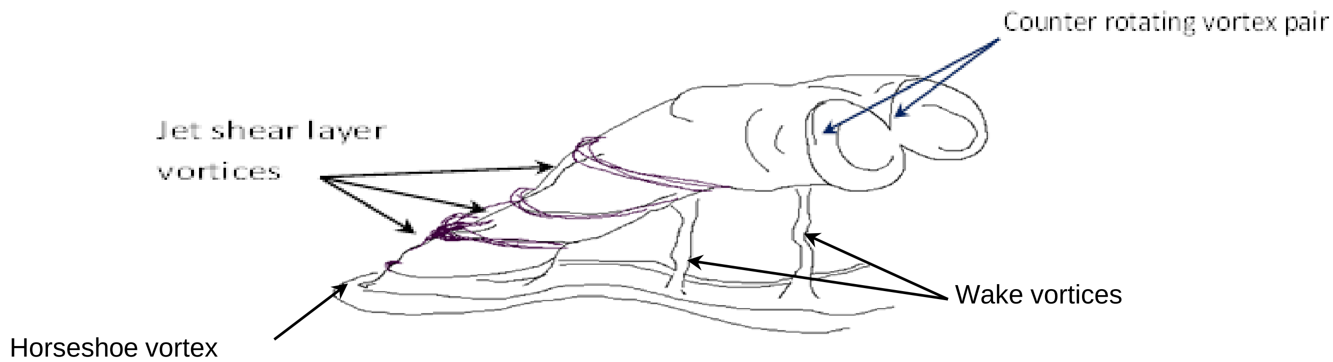


Four coherent structures

- *Shear-layer (Kelvin-Helmoltz vortices)*
- *Horseshoe vortices*
- *Wake vortices*
- *Counter rotating vortex pair (CVP)*

# From a real combustor to a baseline lab configuration: the test bench MAVERIC

Short term objective:

– Providing an experimental database with forcing and relevant conditions: non circular hole geometry and non conformal jet exit section with an acoustic forcing of the crossflow. This experimental database is meant to be first for RANS/DNS/LES assessment.

Long term objective :

– improving the understanding of the effect of the presence of the forcing may have on the unsteadiness of adiabatic cooling efficiency. Identifying optimal hole shapes (if any) compatible with the existing manufacturing process.

# From a real combustor to a baseline lab configuration: the test bench MAVERIC

" With the acoustic forcing system

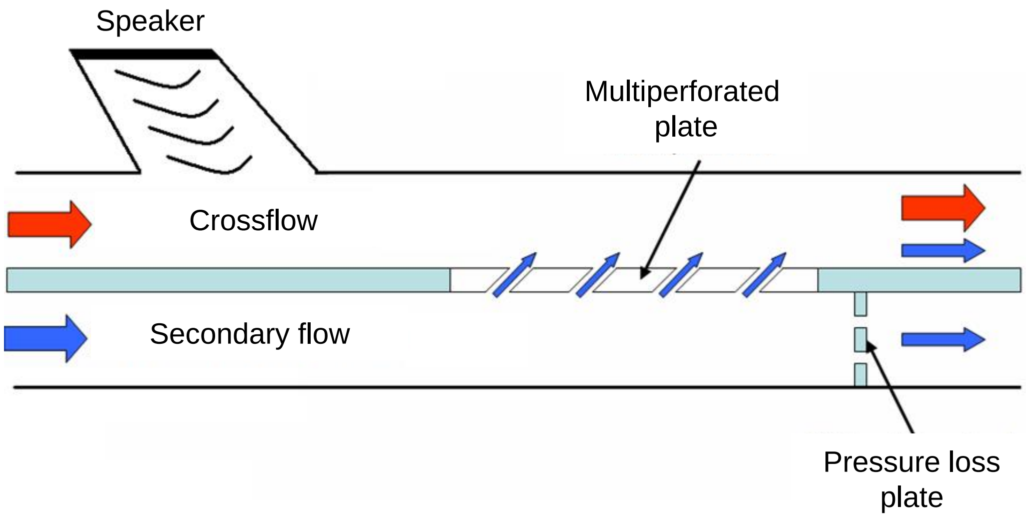


**Analysis of test bench acoustic response**

➔ **Development of data acquisition system and forcing system (LABVIEW)**

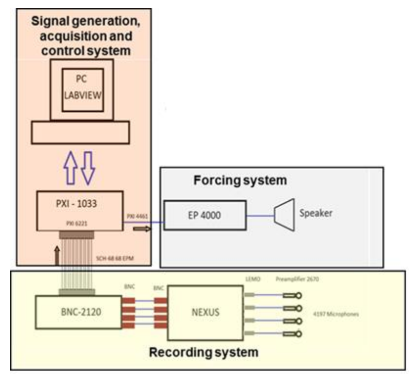


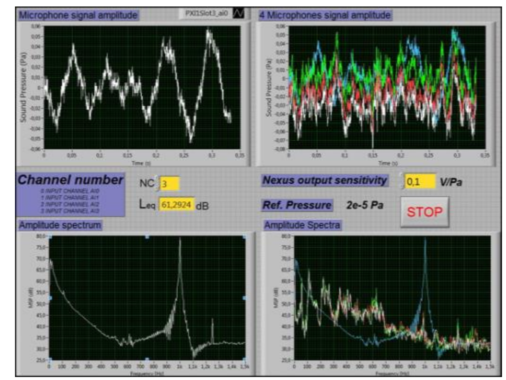


➔ **Setting-up of automatic displacement system for optic measurement tools.**

➔ **<u>Laser Doppler Velocimetry </u>(LDV) & <u>Phase-Locked Particle image Velocimetry </u>(PIV) measurements**

# From a real combustor to a baseline lab configuration: the test bench MAVERIC

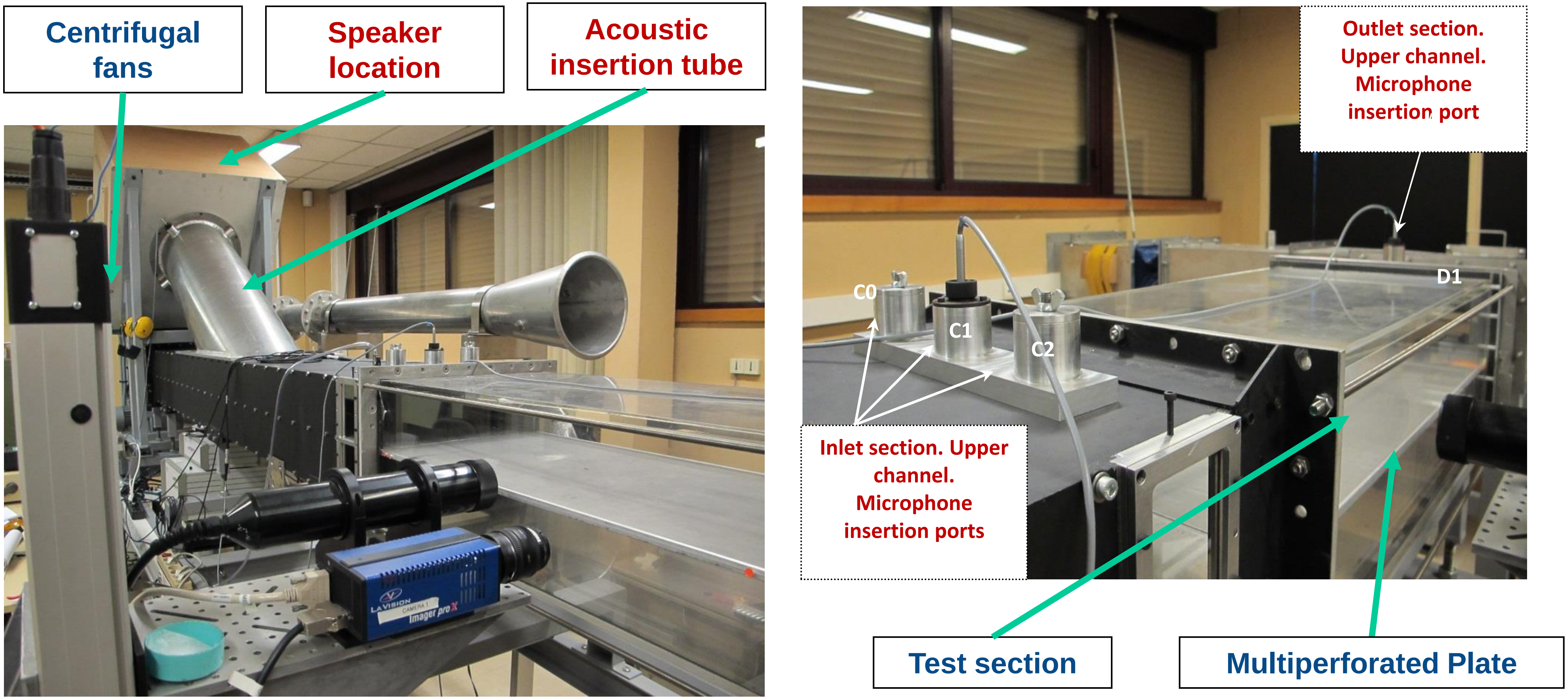


- Pressure drop between lower and upper channel [10 – 140] Pa
- Main stream Reynolds number [2000 – 35000]
- Jet Reynolds number [1200 – 9000]

# Acoustic forcing: Experimental evidence of the flow response.

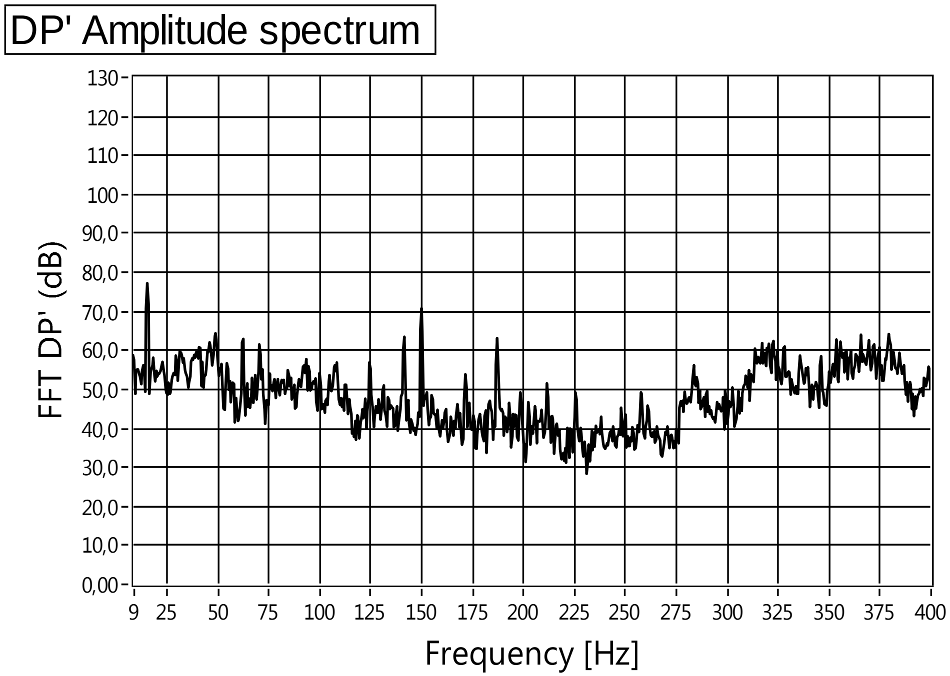


No forcing

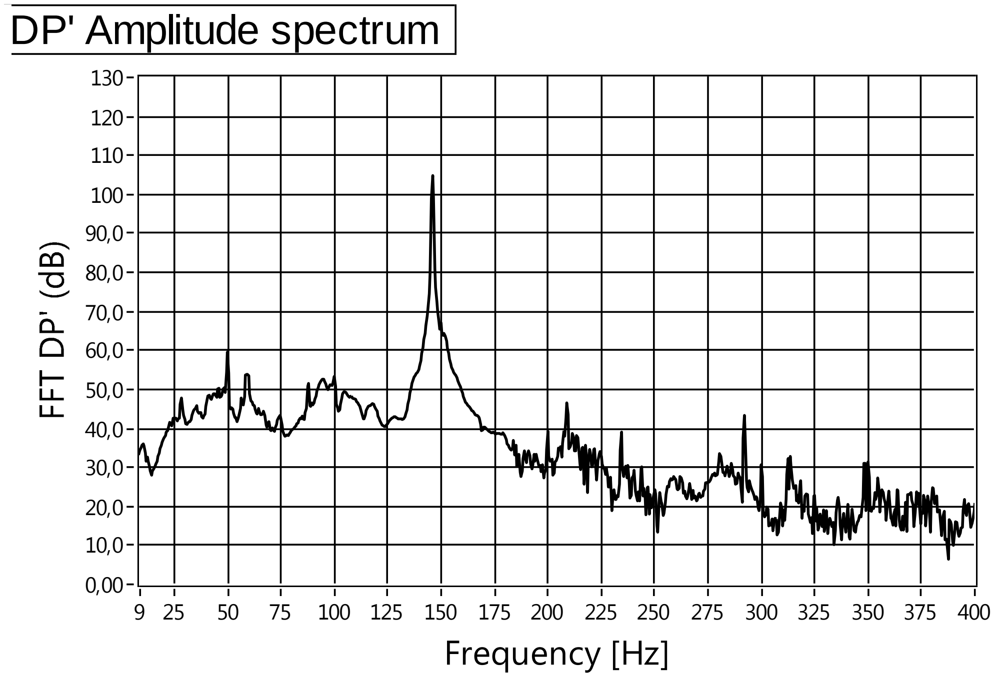


Forcing @146 Hz

SPECTRA OF THE UPSTREAM PARIETAL PRESSURE DIFFERENCE

# Acoustic forcing: Experimental evidence of the flow response.

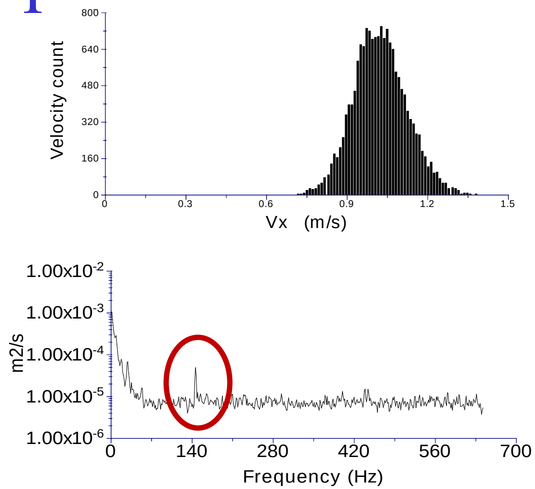


$DP'_{ac} = 12$ Pa

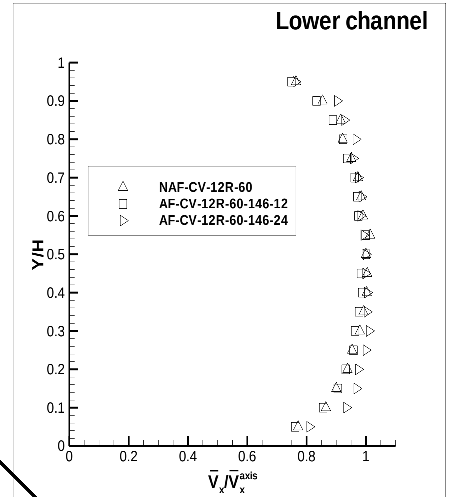


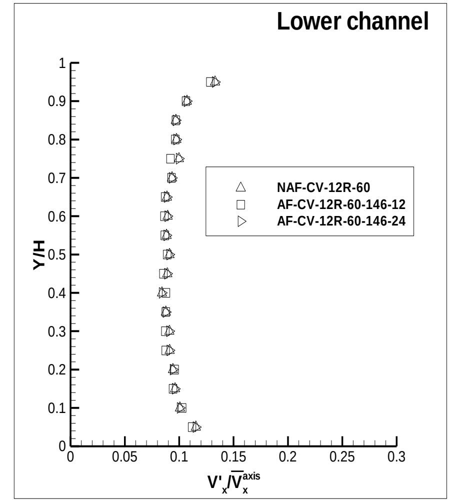


Streamwise velocity component spectra (right) and the ir related histograms (left) in the inlet upper channel

$@\ X_1^* = -22.1$ and $Y^* = 0.5$

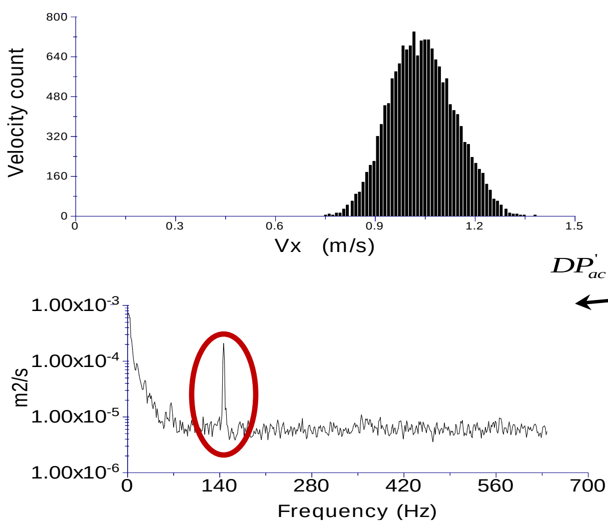


$DP'_{ac} = 24$ Pa

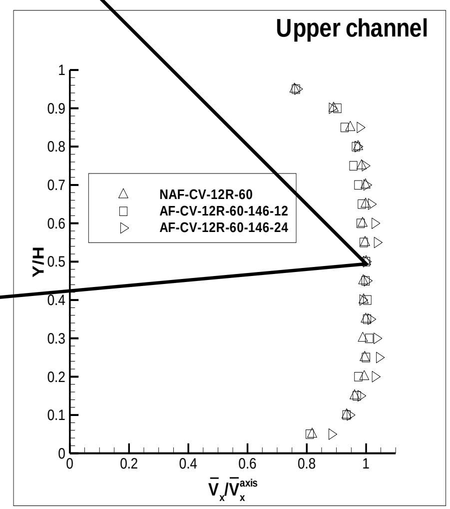


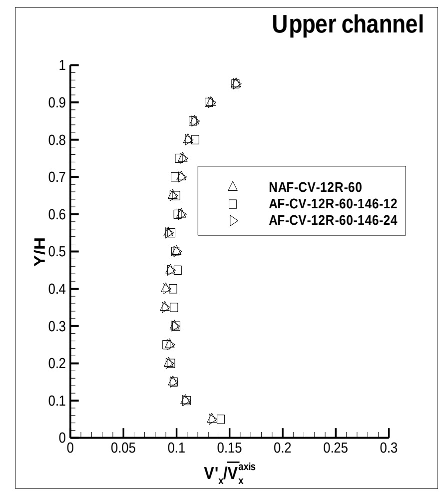

# Acoustic forcing: Experimental evidence of the flow response.

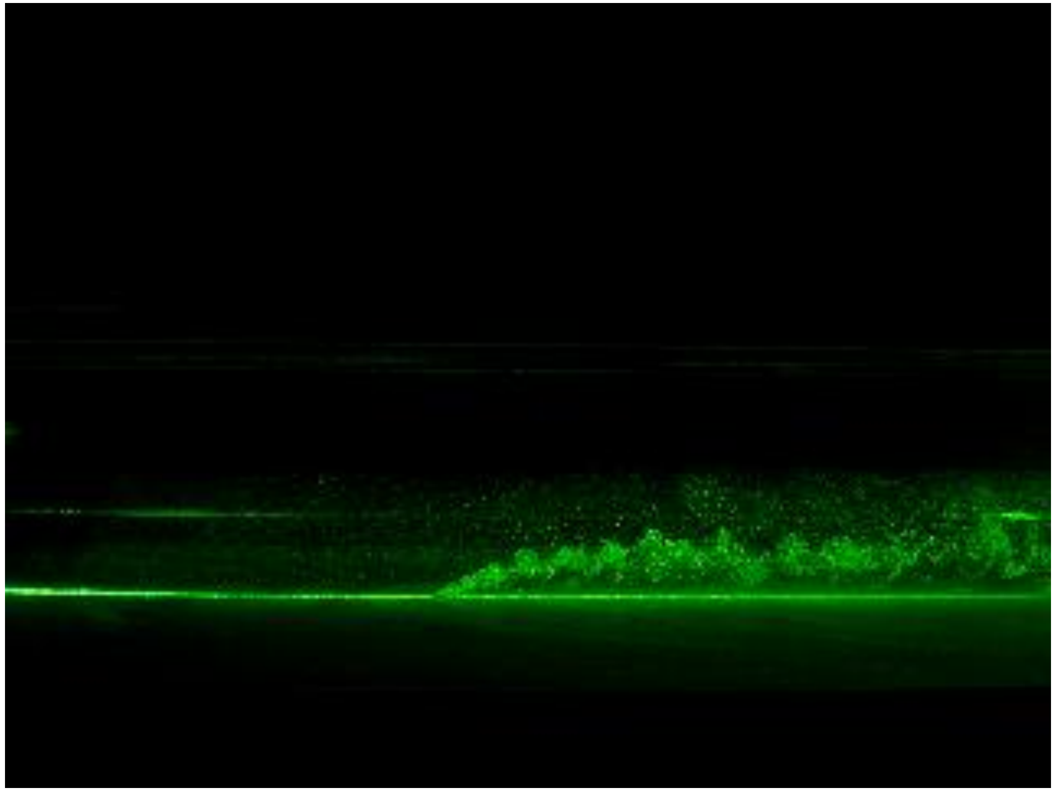

VISUALIZATION TO GET A FLAVOUR OF THE JICF (1-HOLE PLATE WITH FORCING @146 HZ)

# Acoustic forcing: Experimental evidence of the flow response.

Examples of extraction of the jets' coherent motion:

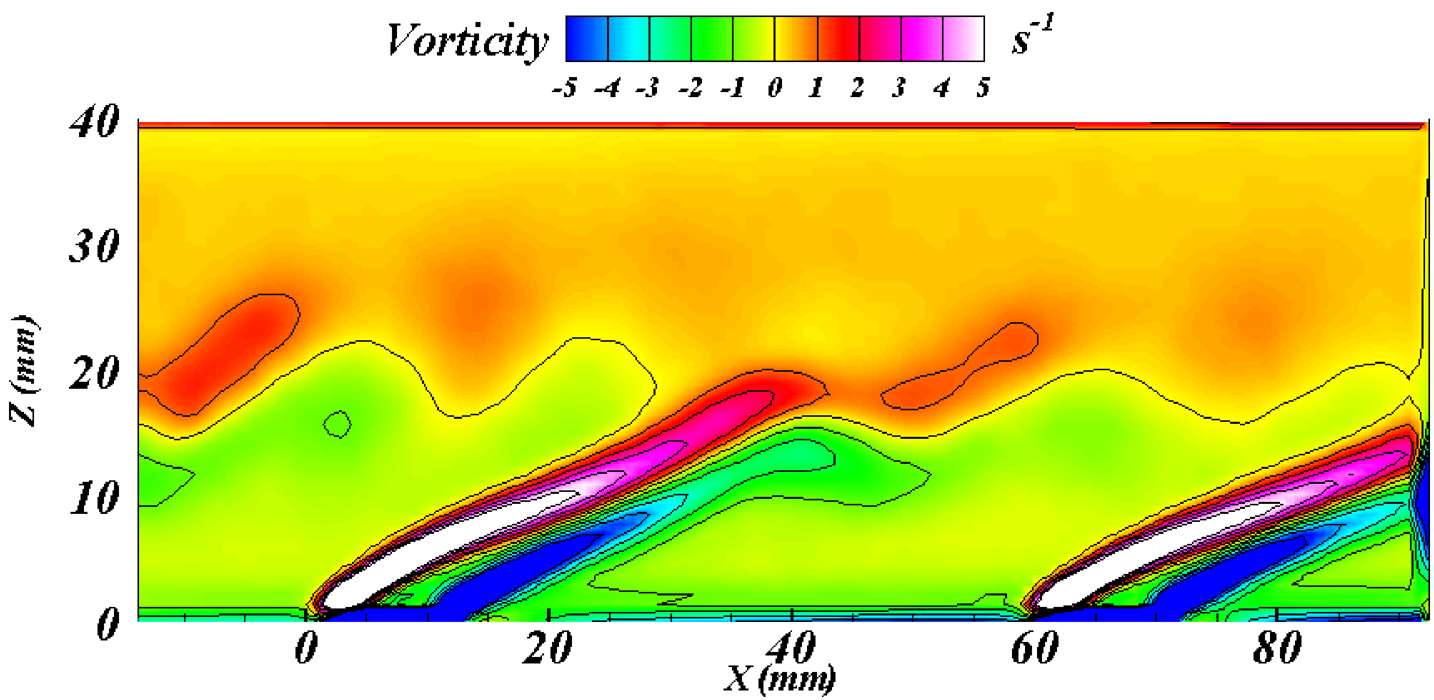


KIAI database - AF-CV-12R-60-146-24 , central jet of rows 3 and 5: phase average time variation incorporating four phase locked averages (0°, 90 °, 180° and 270°, (statistics over 600 images per phase angle).

# Acoustic forcing: Experimental evidence of the flow response.

If the relative intensity of the forcing is inscreased by reducing the mean pressure drop from 60 Pa to 15 Pa

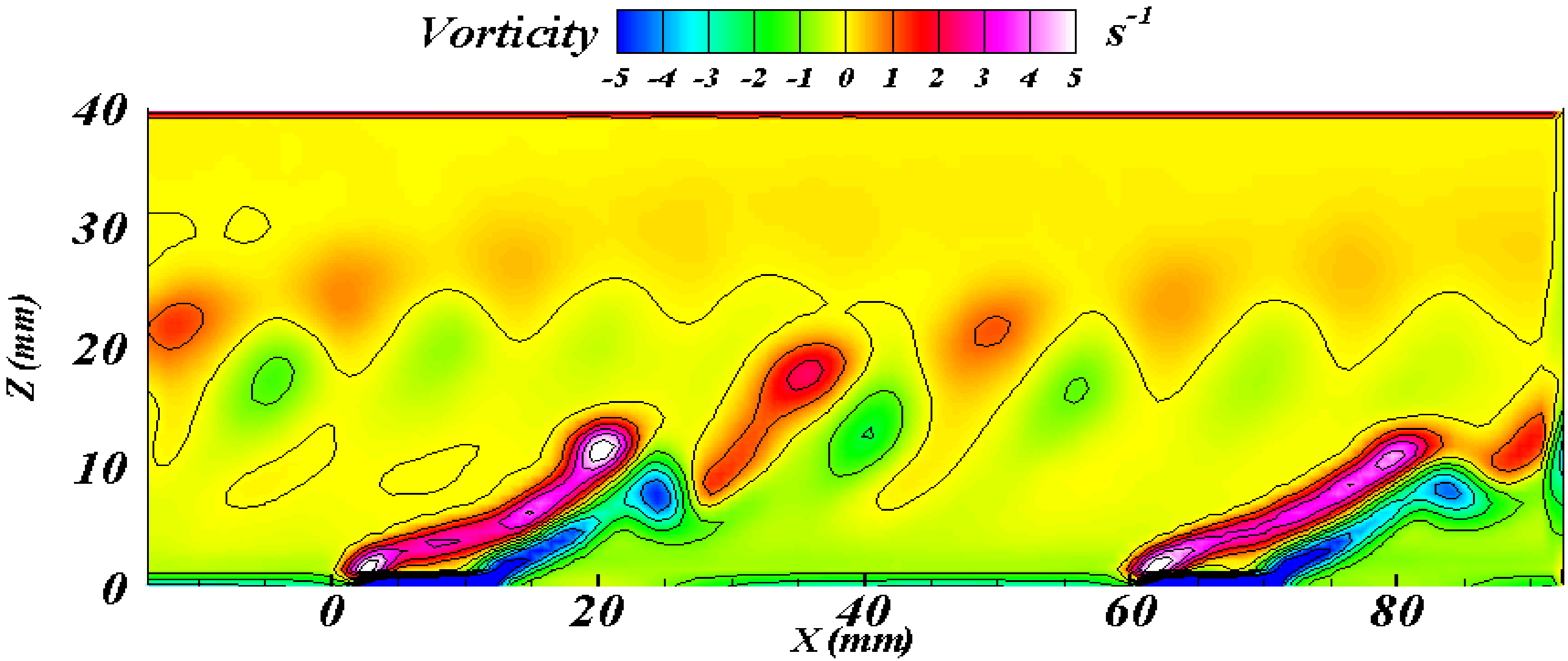


KIAI database - AF-CV-12R-15-146-24 , central jet of rows 3 and 5: examples of extraction of the jet coherent motion: phase average time variation incorporating four phase locked averages (0°, 90 °, 180° and 270°, (statistics over 600 images per phase angle).

# Low Mach flow simulations : AUSM-IT, a discrete flux scheme for a low order FV colocated method

# The continuous system of PDE's: Euler equations

$$\frac{\partial \rho}{\partial t} + \nabla.(\rho \boldsymbol{u}) = 0$$

$$\frac{\partial \rho \boldsymbol{u}}{\partial t} + \nabla.(\rho \boldsymbol{u} \otimes \boldsymbol{u}) = -\nabla p$$

$$\frac{\partial \rho E}{\partial t} + \nabla.(\rho \boldsymbol{u} H) = 0$$

$$E = e + \frac{1}{2}\|\boldsymbol{u}\|^2 = c_v T + \frac{1}{2}\|\boldsymbol{u}\|^2 ; H = E + \frac{p}{\rho}$$

$$p = (\gamma - 1)\rho e$$

Together with proper initial and boundary conditions

# Context and simplifying assumptions

Cell centered finite volume method with variables' co-location on the domain $D = \bigcup_{i=1}^{i=N_{cell}} V_i$ , coordinate system $Ox$ and normal basis $B = [\boldsymbol{e}_1]$.

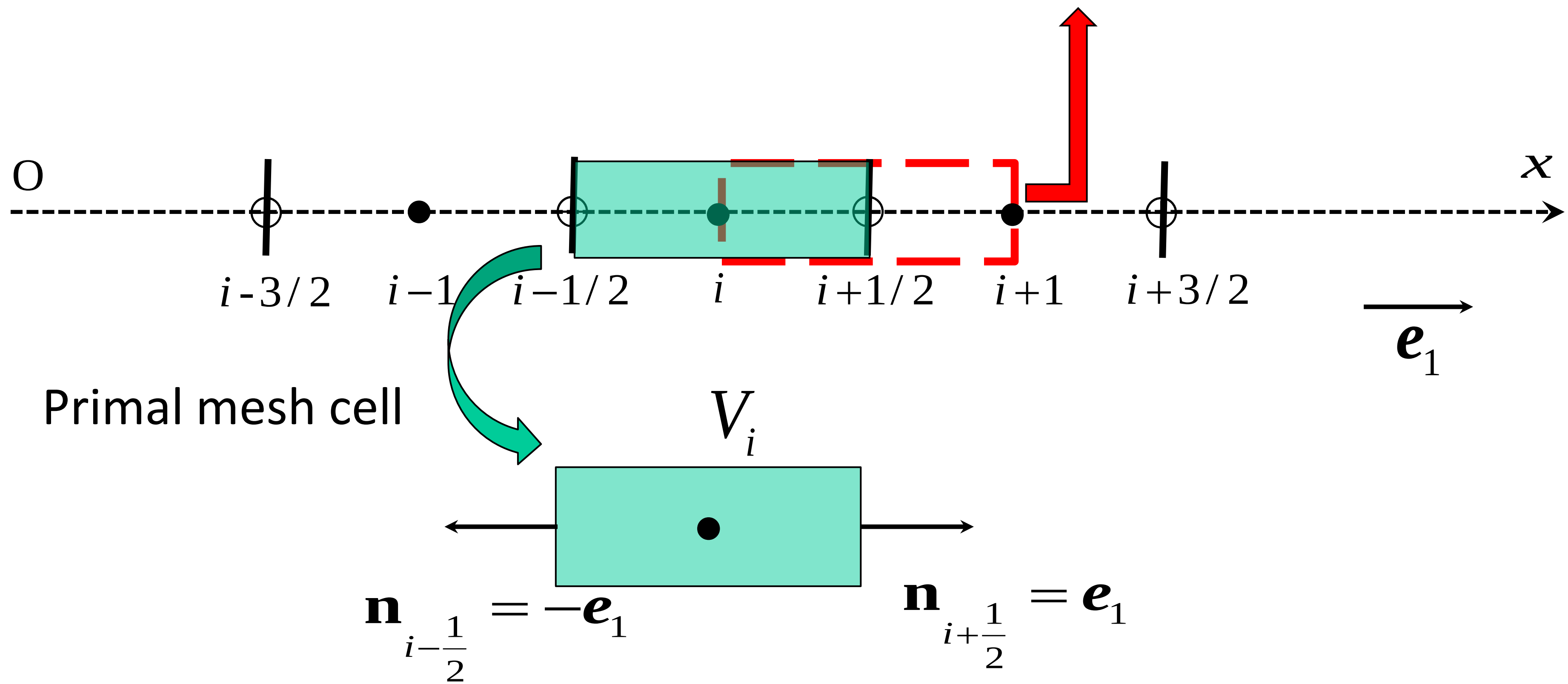

# Expression of the fluxes at the interfaces: momentum equation

Consider a first order Euler implicit time discretization.

Thus, the discrete system at time $t_{n+1} = (n+1)\Delta t$ reads as:

$$\left(\rho u\right)_i^{n+1} \simeq \left(\rho u\right)_i^{n} - \frac{\Delta t}{\left(x_{i+1/2} - x_{i-1/2}\right)}\left[\left(\rho uu\right)_{i+1/2}^{n+1} - \left(\rho uu\right)_{i-1/2}^{n+1} + \left(p\right)_{i+1/2}^{n+1} - \left(p\right)_{i-1/2}^{n+1}\right]$$

So, expressions for the transporting velocities and the face pressure have to be derived. To handle this for the transporting velocity, there is broadly speaking two different alternatives:

# Expression of the fluxes at the interfaces

1. Either you assume that the transporting velocity is given a **dynamical meaning** and so consider that it satisfies an evolution equation obtained by discretizing the continuous momentum equation on the dual mesh → this is the starting point of the **momentum interpolation method**,

2. Or you solve a **Riemann problem** derived from the charateristics system written at the interface between two adjacent control volumes (**Godunov type schemes**) .

# Momentum interpolation method

For the flux of momentum, let's re-write it formally as :

$\left(\rho uu\right)_{i-1/2}^{n+1} = \left(\rho u\right)_{i-1/2}^{n+1} u_{i-1/2}^{n+1}$ and conversely $\left(\rho uu\right)_{i+1/2}^{n+1} = \left(\rho u\right)_{i+1/2}^{n+1} u_{i+1/2}^{n+1}$

Then, consider that $\left(\rho u\right)_{i\pm1/2}^{n+1}$ is the sought **transported** quantity

and that $u_{i\pm1/2}^{n+1}$is the **transporting** velocity. On the ground of the sole

discretization on the primal cell, $u_{i\pm1/2}^{n+1}$ can be thought of as

an interpolated quantity based on the cell based values .

We shall denote it by $u_{i\pm1/2}^{*,n+1} = Interp\left(u_i^{n+1}, u_{i\pm1}^{n+1}\right)$.

# Momentum interpolation method

Then we make the following approximations:

1) The transporting velocity is treated explicitly in time so $u_{i\pm1/2}^{*,n+1} \approx u_{i\pm1/2}^{*,n}$

2) An upwind first order expression in space is retained for the transported quantity.

So one gets the following expressions (positive velocities):

$$\left(\rho uu\right)_{i-1/2}^{n+1} \approx \left(\rho u\right)_{i-1}^{n+1} u_{i-1/2}^{*,n} \overset{notation}{\equiv} B_i$$

$$\left(\rho uu\right)_{i+1/2}^{n+1} \approx \left(\rho u\right)_{i}^{n+1} u_{i+1/2}^{*,n} \overset{notation}{\equiv} \left(\rho u\right)_{i}^{n+1} A_i = B_{i+1}$$

# Momentum interpolation method

So, the $B_i$'s stand for the momentum flux at the interfaces of the primal mesh and the $A_i$'s stand for the transporting velocities therein, so with these notations, the discretized momentum equation on a primal mesh cell reads now as:

$$(\rho u)_i^{n+1} = (\rho u)_i^n - \frac{\Delta t}{\Delta x}\left[(\rho u)_i^{n+1} A_i - B_i + (p)_{i+1/2}^{n+1} - (p)_{i-1/2}^{n+1}\right]$$

or equivalently:

$$B_i = (\rho u)_i^{n+1} A_i + (p)_{i+1/2}^{n+1} - (p)_{i-1/2}^{n+1} + \frac{\Delta x}{\Delta t}\left[(\rho u)_i^{n+1} - (\rho u)_i^n\right] \text{ or}$$

$$B_i = B_{i+1} + (p)_{i+1/2}^{n+1} - (p)_{i-1/2}^{n+1} + \frac{\Delta x}{\Delta t}\left[(\rho u)_i^{n+1} - (\rho u)_i^n\right]$$

# Momentum interpolation method: primal mesh view

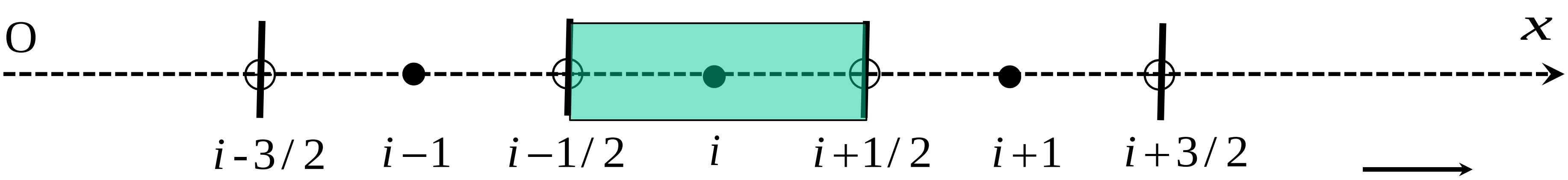


Primal mesh cell

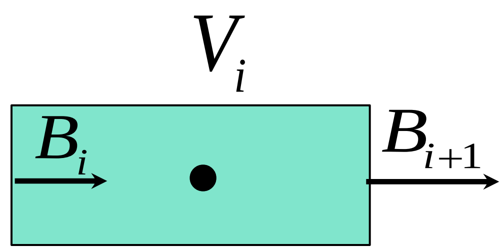


$$B_{i+1} = A_i \times (\rho u)_i$$

# Momentum interpolation method: dual mesh equation

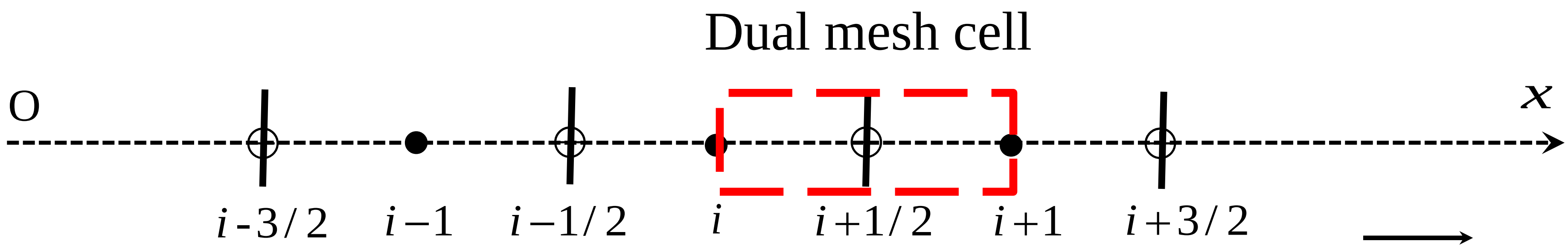


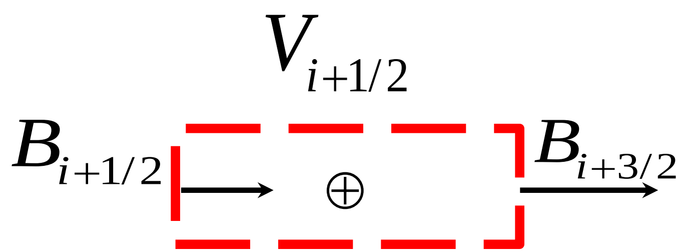


$$B_{i+3/2} = A_{i+1/2} \times (\rho u)_{i+1/2}$$

The same type of discretized momentum equation is postulated on the dual mesh, namely:

$$B_{i+1/2} = (\rho u)^{n+1}_{i+1/2} A_{i+1/2} + (p)^{n+1}_{i+1} - (p)^{n+1}_{i} + \frac{\Delta x}{\Delta t}\left[(\rho u)^{n+1}_{i+1/2} - (\rho u)^{n}_{i+1/2}\right]$$

# Momentum interpolation method: relating primal and dual cells quantities

Where $A_{i+1/2}$ and $B_{i+1/2}$ are supposed to be such that (Rhie and Chow, 1993):

$$A_{i+1/2} = 2\,\frac{A_i A_{i+1}}{A_i + A_{i+1}}$$

$$\frac{B_{i+1/2}}{A_{i+1/2}} = \frac{1}{2}\left(\frac{B_i}{A_i} + \frac{B_{i+1}}{A_{i+1}}\right)$$ which leads to:

$$(\rho u)_{i+1/2}^{n+1} = \frac{1}{2}\left[\frac{(\rho u)_{i-1}^{n+1} u_{i-1/2}^{*,n}}{u_{i+1/2}^{*,n}} + \frac{(\rho u)_{i}^{n+1} u_{i+1/2}^{*,n}}{u_{i+3/2}^{*,n}}\right] - \frac{1}{A_{i+1/2}}\left[(p)_{i+1}^{n+1} - (p)_{i}^{n+1}\right]$$

$$-\frac{1}{A_{i+1/2}}\frac{\Delta t}{\Delta x}\left[(\rho u)_{i+1/2}^{n+1} - (\rho u)_{i+1/2}^{n}\right]$$

# Momentum interpolation method: the final expression of the primal cell face velocity

$$(u)_{i+1/2}^{n+1} = (\rho u)_{i+1/2}^{n+1} / \rho_{i+1/2}^{n+1} \text{ where } \rho_{i+1/2}^{n+1} = \frac{1}{2}\left[\rho_i^{n+1} + \rho_{i+1}^{n+1}\right]$$

and the $\rho_i^{n+1}$ are calculated through the continuity equation discretized as the momentum on the primal mesh.

We are done with the interface velocity on the primal mesh but not with the pressure interface ! To calculate the latter, an AUSM$^+$ expression is used (Liou, 1996), :

$$(p)_{i+1/2}^{n} = f_p^+(M_i)(p)_i^n + f_p^-(M_{i+1})(p)_{i+1}^n \text{ with:}$$

$$f_p^{\pm}(M) = \frac{1}{4}(M \pm 1)^2(2 \mp M) \pm \frac{3}{16}M\left(M^2 - 1\right)^2 \text{ with } |M| < 1$$

# Momentum interpolation method: example of results for a 2D pulse simulations (second order discretization, from Moguen et

Initial conditions:

$$\rho(x,y,t=0)=\rho_0+\delta\rho$$

$$u(x,y,t=0)=u_0$$

$$v(x,y,t=0)=v_0$$

$$p(x,y,t=0)=p_0+\delta p$$

$$\delta p = 200\exp\left[-\frac{(x-0.5)^2+(y-0.5)^2}{0.05^2}\right]$$

and $\delta\rho=\delta p / c_0^2$ with $c_0^2=\gamma p_0/\rho_0$

$M_0 \approx 10^{-5}$, mesh size 500 x 500,

domain size 1m x1m

Acoustic CFL number : 20

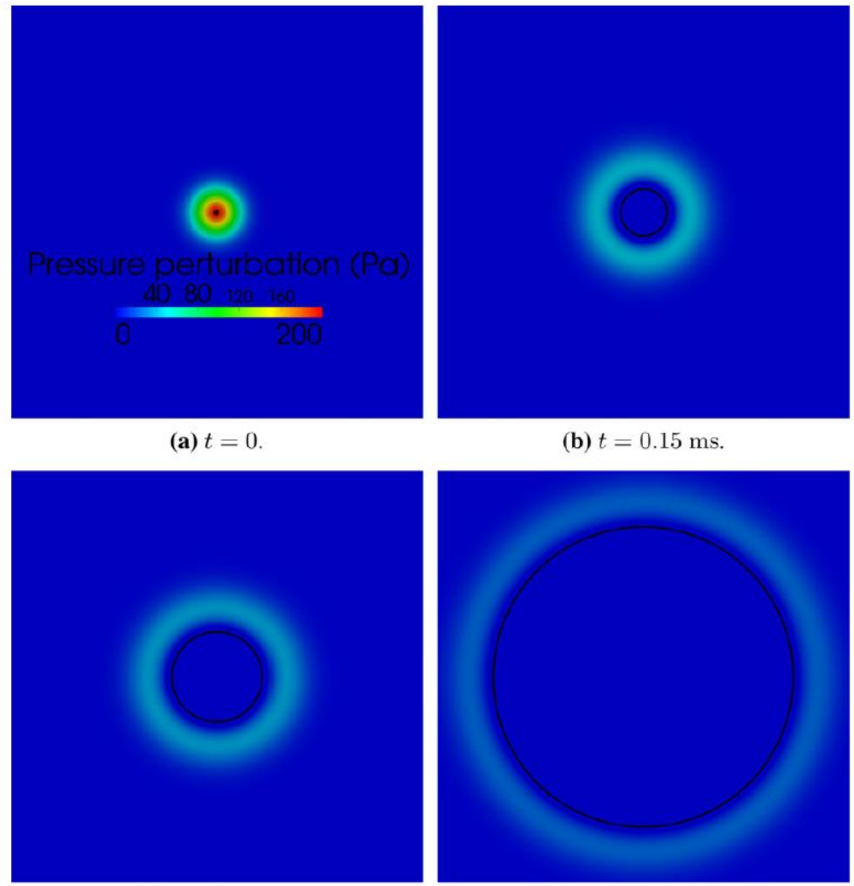


**(a)** $t=0.$ **(b)** $t=0.15$ ms. **(c)** $t=0.30$ ms. **(d)** $t=1.00$ ms.

$$\varrho_0 = 1.2046\,\mathrm{kg\,m^{-3}},\quad u_0=v_0=0.30886 10^{-2}\,\mathrm{m\,s^{-1}},\quad p_0=101300\,\mathrm{Pa}$$

# Evolution of the momentum interpolation method for low Mach number Riemann problem (from Moguen et al., 2015a)

**Table 1**
Low Mach number acoustic Riemann problem with a two-shock solution.

| $\varrho_L$ (kg/m$^3$) | $v_L$ (m/s) | $p_L$ (Pa) | $\varrho_R$ (kg/m$^3$) | $v_R$ (m/s) | $p_R$ (Pa) |
|---|---|---|---|---|---|
| 25 | 0.6 | 14 000 | 25 | 0.2 | 14 000 |

Dispersion Effect !

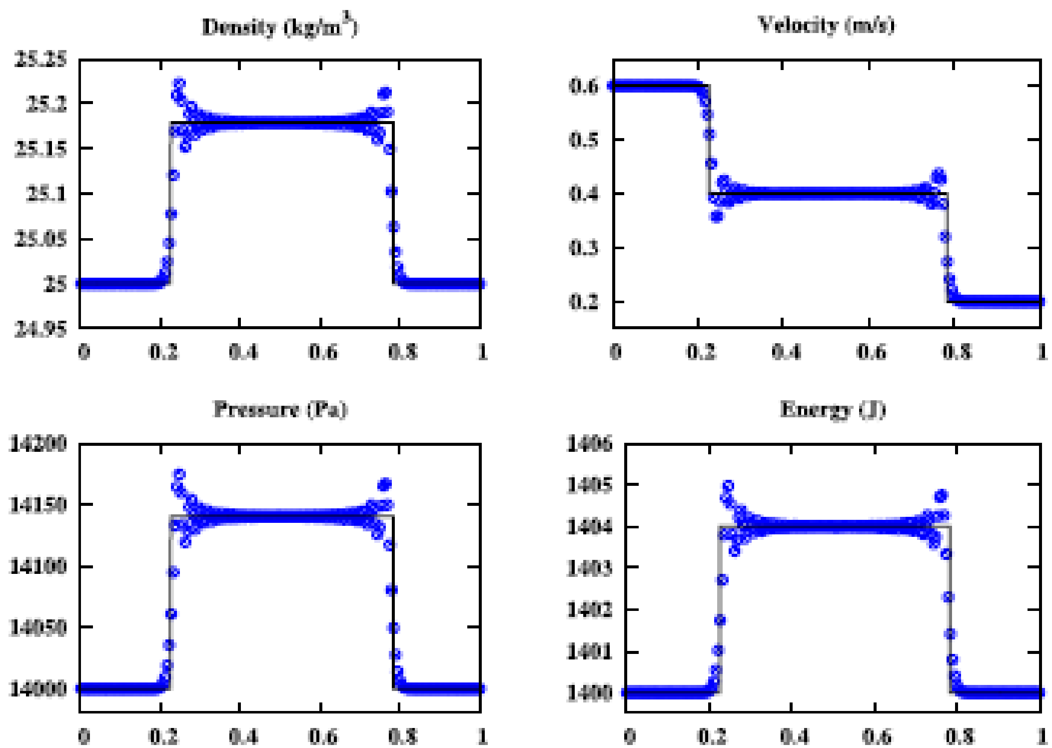


**Fig. 1.** Low Mach number acoustic Riemann problem with a two-shock solution (cf. Table 1), second-order discretization [7]. Rhie–Chow momentum interpolation solution (○), cf. Eq. (5), vs. exact solution (solid line) at time $t = 0.01$ s.

# Evolution of the momentum interpolation method for low Mach number Riemann problem (from Moguen et al., JCP, 2015a)

Centering the velocity in the face velocity expression

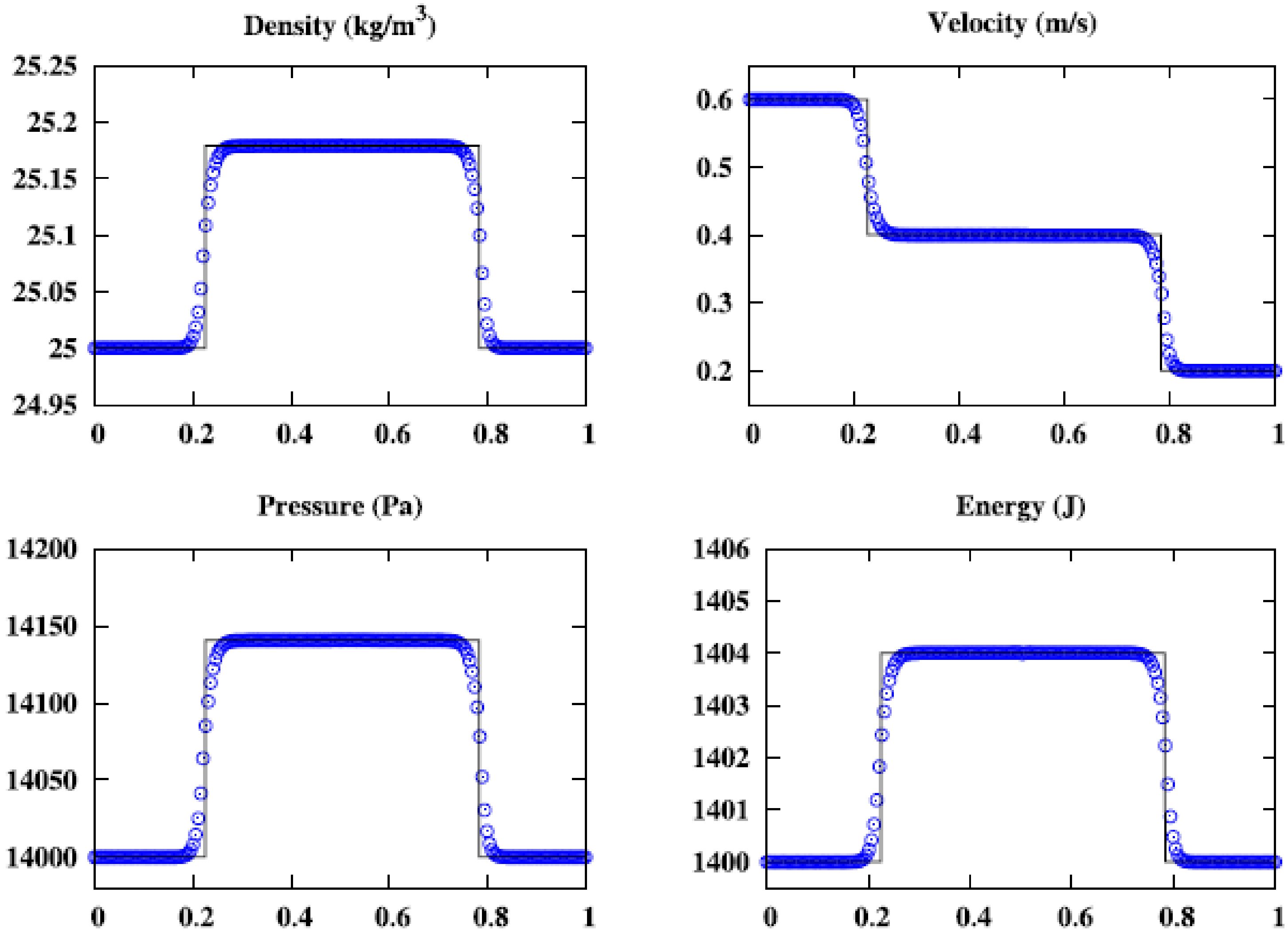

## Using the momentum interpolation as a guide to improve a Godunov type scheme (from Moguen et al., JCP, 2015b) for low Mach number

AUSM$^+$-up mass flux (Liou, 2006)

$$(\varrho v)_{i+1/2} = (\varrho c M)_{i+1/2} - \frac{K_p \max\{1-\sigma \overline{M}^2, 0\}}{c_{i+1/2} f_c(M_0)} (p_{i+1} - p_i),$$

Mimicking the form obtained when using the momentum interpolation method

AUSM-IT (IT : Inertia Term) mass flux (Moguen et al., 2015a)

$$(\varrho v)_{i+1/2}^{n+1} = (\varrho c M)_{i+1/2}^{n+1} - \frac{K \max\{1-\sigma \overline{M}^2, 0\}}{c_{i+1/2}^{n+1} f_c(M_0)} \left\{ p_{i+1}^n - p_i^n + \underline{\frac{\Delta x}{\Delta t} \left[ (\varrho v)_{i+1/2}^{n+1} - (\varrho v)_{i+1/2}^n \right]} \right\}$$

# Beneficial effect: the correct low Mach asymptotic behavior at the discrete level is recovered.

- Setting

$$\mathrm{M} = v_{\mathrm{ref}} / \sqrt{p_{\mathrm{ref}}/\varrho_{\mathrm{ref}}}$$

$$\varrho = \varrho_{\mathrm{ref}}(\varrho^{(0)} + \mathrm{M}\varrho^{(1)} + \mathrm{M}^2\varrho^{(2)} + \ldots)$$

$$v = v_{\mathrm{ref}}(v^{(0)} + \mathrm{M}v^{(1)} + \mathrm{M}^2 v^{(2)} + \ldots)$$

$$p = p_{\mathrm{ref}}(p^{(0)} + \mathrm{M}p^{(1)} + \mathrm{M}^2 p^{(2)} + \ldots)$$

- $\xi = \mathrm{M}x$ (variable for the large acoustic length scale)
$\varrho^{(l)} = \varrho^{(l)}(x, \xi, t)$, $v^{(l)} = v^{(l)}(x, \xi, t)$, $p^{(l)} = p^{(l)}(x, \xi, t)$, $l = 0, 1, 2$
- Substitution of the expansions in the Euler equations and averaging on the small convective length scale leads to the acoustic wave equation :

$$\partial_t \widetilde{v^{(0)}} + \partial_\xi p^{(1)} / \varrho^{(0)} = 0$$

$$\partial_t p^{(1)} + \gamma p^{(0)} \partial_\xi \widetilde{v^{(0)}} = 0$$

# The discrete (at first order) acoustic energy level is conserved with AUSM-IT

- Substituting $\widetilde{v^{(0)}}$ and $p^{(1)}$ into the low Mach number form of the AUSM-IT scheme :

$$v_{i+1/2} = \frac{v_i + v_{i+1}}{2} - \frac{1}{2(\varrho c)_{i+1/2}\mathrm{M}_\mathrm{r}^2}(p_{i+1} - p_i) - \frac{\mathrm{St}_\mathrm{r}\,\Delta x}{2c_{i+1/2}\mathrm{M}_\mathrm{r}}\partial_t v_{i+1/2}$$

$$p_{i+1/2} = \frac{p_i + p_{i+1}}{2}$$

and setting $\Delta\xi = \mathrm{M}_\mathrm{r}\Delta x$ ($\Delta x$ at the convective length scale), the equivalent equation for $p^{(1)}$ (2nd order error) is :

$$\mathrm{St}_\mathrm{r}\,\partial_t p^{(1)} + \gamma p^{(0)}\nabla_\xi \cdot \widetilde{\boldsymbol{v}^{(0)}} = \frac{c^{(0)}\Delta x}{2\mathrm{M}_\mathrm{r}}\left(\nabla_\xi \cdot \nabla_\xi p^{(1)} + \varrho^{(0)}\mathrm{St}_\mathrm{r}\,\partial_t \nabla_\xi \cdot \widetilde{\boldsymbol{v}^{(0)}}\right)$$

With the equivalent equation for $\widetilde{\boldsymbol{v}^{(0)}}$ (2nd order error), the right-hand side is zero

- Consequence : The acoustic wave equations are retrieved (2nd order error)

# The discrete (at first order) acoustic energy level is conserved with AUSM-IT

Suppose that $\widetilde{\varrho^{(0)}}$ et $c^{(0)}$ are constant in time and space

Acoustic energy ($\mathbb{T}$ : unit torus, assuming periodic boundary conditions) :

$$E_a = \int_{\mathbb{T}} \left[ \frac{1}{2} \widetilde{\varrho^{(0)}} \| \widetilde{\boldsymbol{v}^{(0)}} \|^2 + \frac{1}{2} \frac{(p^{(1)})^2}{\widetilde{\varrho^{(0)}} (c^{(0)})^2} \right]$$

$$\mathrm{d}_t E_a = \widetilde{\varrho^{(0)}} \int_{\mathrm{T}} \widetilde{\boldsymbol{v}^{(0)}} \cdot \partial_t \widetilde{\boldsymbol{v}^{(0)}} + \frac{1}{\widetilde{\varrho^{(0)}} (c^{(0)})^2} \int_{\mathrm{T}} p^{(1)} \partial_t p^{(1)}$$

With the equivalent equations (2nd order error) :

$$\mathrm{d}_t E_a = 0$$

Without an inertia term, acoustic energy is dissipated with the decrease rate :

$$\mathrm{d}_t E_a = - \frac{\Delta x}{2 \, \mathrm{St_r} \widetilde{\varrho^{(0)}} c^{(0)} \mathrm{M_r}} \int_{\mathrm{T}} \| \nabla_{\xi} p^{(1)} \|^2 \leq 0$$

# Behavior of AUSM+-up for propagating wave (inlet velocity forcing): evidence of a quite strong dissipation

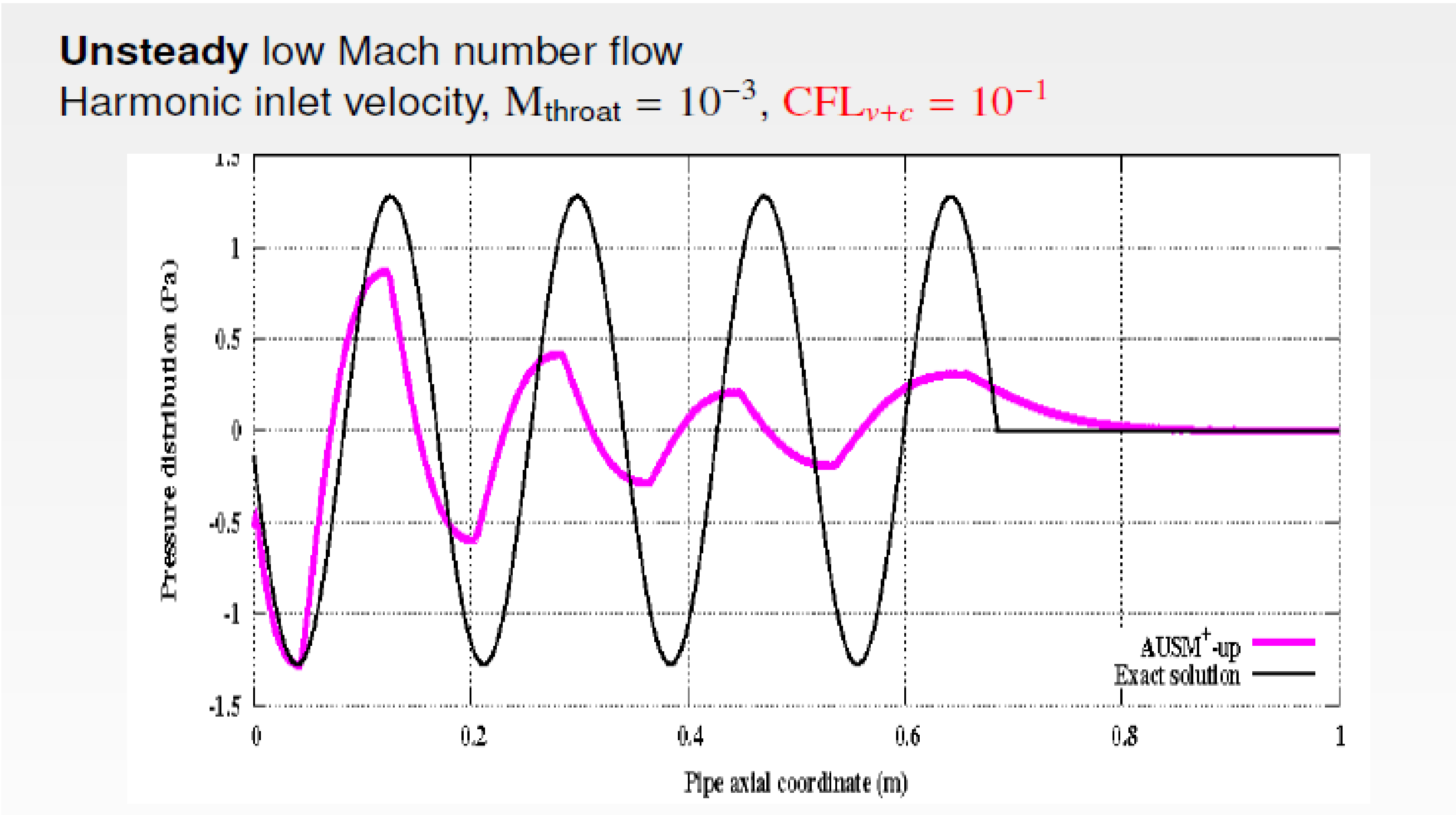

# Behavior with AUSM-IT for the same propagating wave

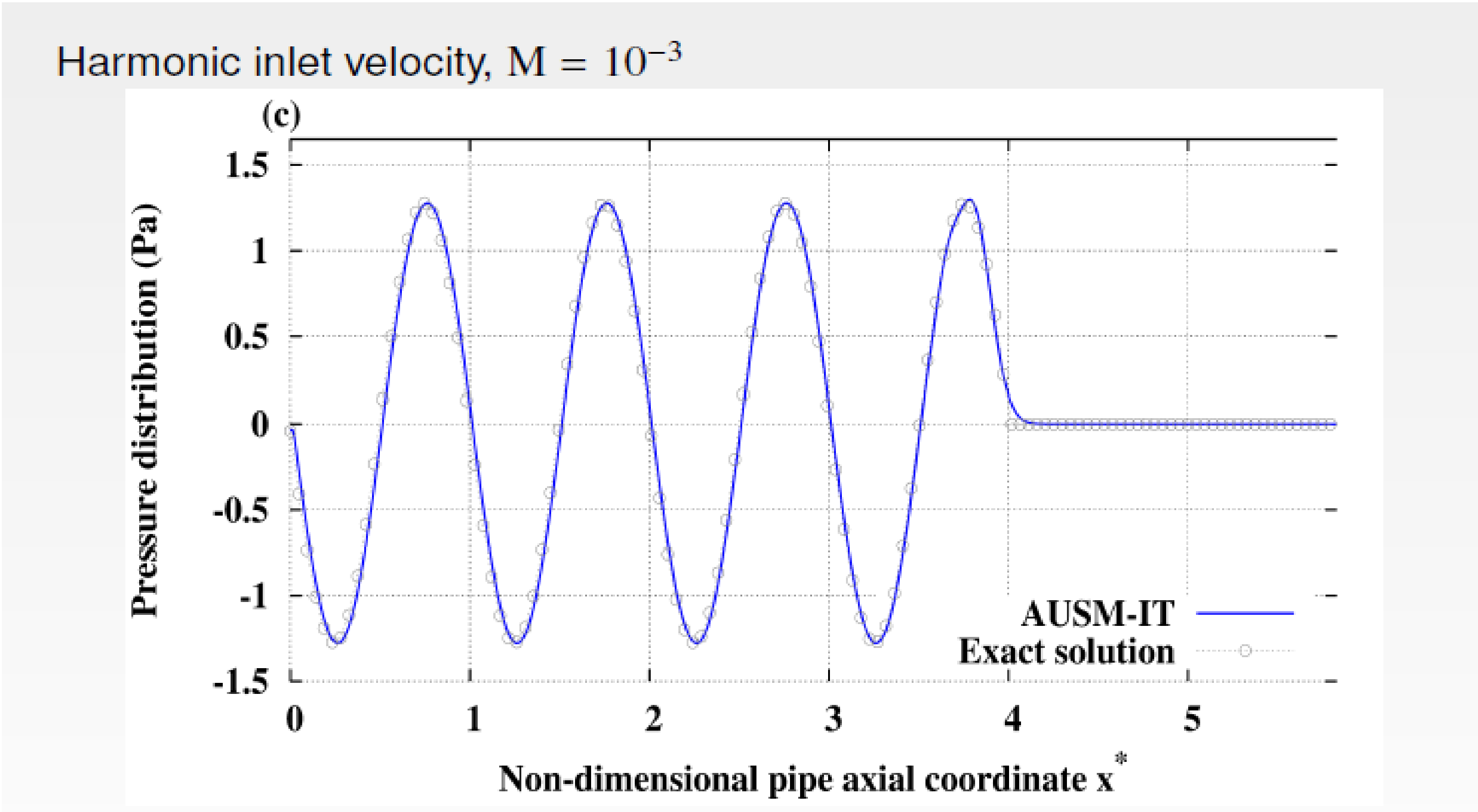

# Low Mach turbulent flow unsteady simulation: ATCBC, a proposal for the boundary condition prescription.

# Brief recap: simulations of turbulent flows

- Option A - Modeling, discretizing, solving (most widely used)
  - **Step A-1** *Turbulence modeling*
    - **Reynolds Averaged Navier-Stokes (RANS)** - Unconditional NS ensemble averaging (temporal filtering over all time scales of fluctuations if ergodicity property is fulfilled). The resulting solution is a **steady** averaged solution.
    - **Unsteady Reynolds Averaged Navier Stokes (URANS) -** Ensemble conditional averaging at a continuously varied given phase angle of a coherent mono-harmonic motion, artificially introduced (forcing) or naturally present in the flow. The unsteadiness is that of conditionnally **averaged** fields (Phase locking). This is directly related to the triple decomposition proposed by Hussain and Reynolds (JFM, 1971).
    - **Large-eddy simulations (LES)** - NS space (most of the time) filtering with a compact filter. The resulting 3D **instantaneous** (filtered) flow fields realizations are **unsteady**.

# Brief recap: simulations of turbulent flows

- Option **A** (continued):
  - **Step A-2** *Discretization*

    Finite differences, finite volumes, finite elements, high performance computing strategy (**LES**), method of solution (explicit, implicit), mesh generation (structured vs unstructured) management issues (related to HPC) .

  - **Step A-3** *Simulation*

    Run, collect, post-process and analyze the results.

# Brief recap: simulations of turbulent flows

- Option **B** - Discretizing, solving i.e. **DNS** (3D, used for simple geometries and not too high a turbulent Reynolds number):
  - Step **B-1** *Discretization*

Finite differences, finite volumes, finite elements, spectral methods, high performance computing strategy (unavoidable), method of solution (explicit, implicit), mesh generation (structured vs unstructured) and management issues (related to HPC).

  - Step **B-2** *Simulation*

Run, collect (a real issue !!), post-process and analyze the results.

This is the purpose of the AeroSol Library developed by the Cagire team (in partnership with Cardamon Inria team)

# Prescribing boundary conditions for low Mach flow simulations

To determine the **number of physical boundary conditions** to be imposed, the guide is the **wave pattern system analysis** at the considered boundary. The sign of the eigenvalues of the Euler flux jacobian matrix and their multiplicity order is the guide (Poinsot and Lele, 1992)

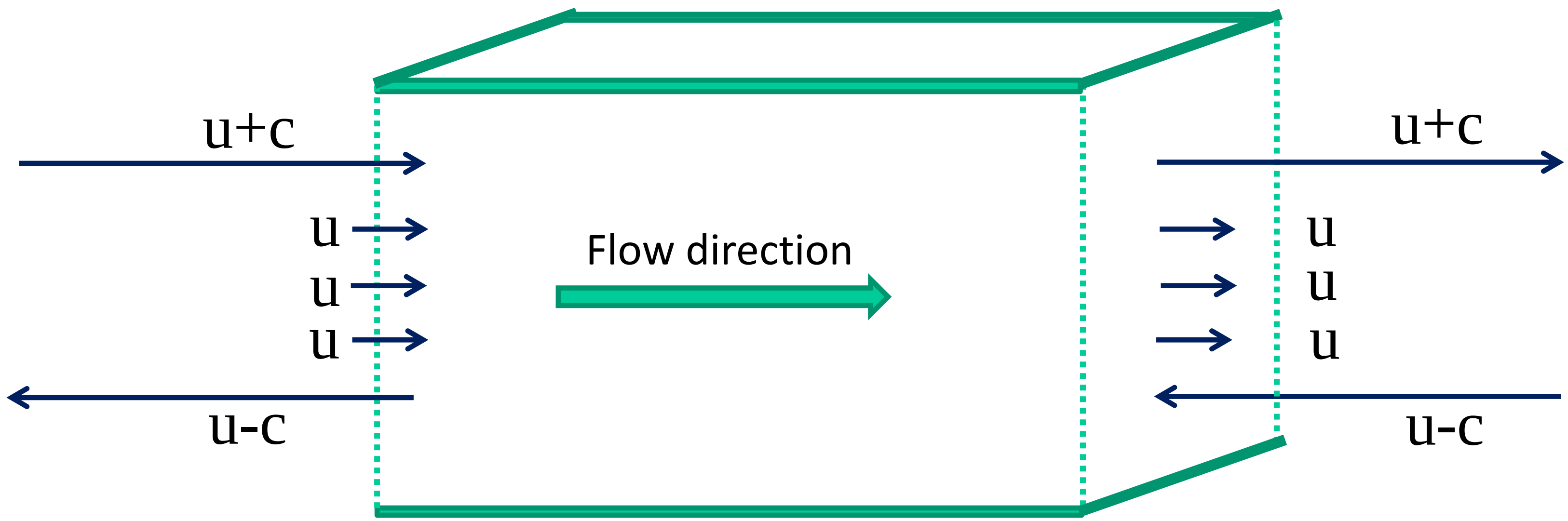

# Prescribing boundary conditions for low Mach flow simulations

The combinations are numerous, see Poinsot and Lele (JCP, 1992) for more details about well posedness vs implementation feedback

Number of physical boundary conditions @inlet for inert NS
(Practically: 4 imposed)
A possible set is:

$$u(t) = \overline{u} + u'(t)$$
$$v(t) = 0 + v'(t)$$
$$w(t) = 0 + w'(t)$$
$$T_t = T_s \times \left(1 + \frac{\gamma - 1}{2} M^2\right)$$

If needed, p is extrapolated from the interior domain.

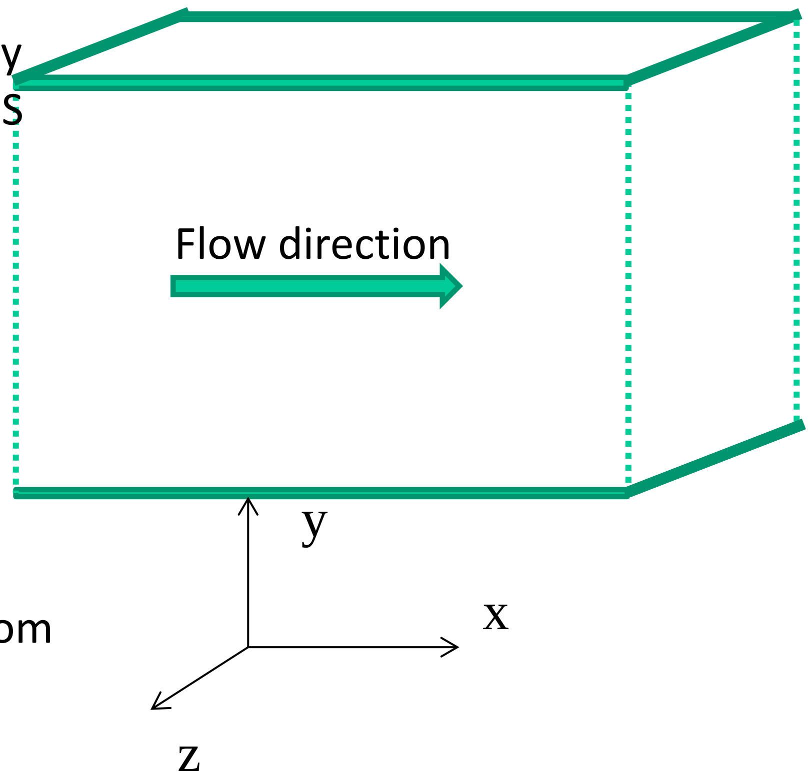


Number of physical boundary conditions @outlet for inert NS,
(Practically 4 imposed)
1 Euler like + 3 viscous
A possible set:
Static pressure imposed @infinity and three viscous conditions (zero normal derivative of $\tau_{xy}$, $\tau_{xz}$ and of the normal heat flux)

## At the inlet, how to generate $u'(x,t), v'(x,t), w'(x,t)$ ?

- **Approach:** choice of the triple decomposition proposed by Hussain and Reynolds (1970)

$$u'(t) = u'_p(t) + u'_s(t) \quad \text{(assuming that } \overline{u'_p u'_s} = 0\text{)}$$

Question: how can $u'_p(t)$ and $u'_s(t)$ be generated ?

$u'_p(t)$ is deterministic so it is quite easy, but $u'_s(t)$ is not.

# At the inlet, how to generate $u_s^{'}(x,t)$ ?

**Precursor simulation**: perform a separate simulation and store the results in a plane that will be used to feed the current simulation (computationaly expansive, simple geometries only)
**Recycling on the fly**: select a plane at some downstream section in the current simulation and regularly reinject the (scaled) values at the inlet (Simple geometries, absence of strong pressure gradients, pb with recycling frequency for aeroacoustics).
**Synthetic turbulence generation (STG)**: white noise, stochastic differential equations, digital filtering, synthetic eddy method (the artificial nature of turbulence leads to long adaptation length, but can be improved).
**Volumic forcing**: add a force in the momentum equation (efficient when combined with STG)
**Vortex generating devices**: simple but provide quite long adaptation length.

(See Shur et al., Flow Turbulence and Combustion 93:63-92 (2014) and the references therein for a more complete overview )

# Example of choice of STG: the synthetic eddy method

Eddy method (SEM): direct injection at the inlet plane of analytically defined structures that reproduce to some extent the coherent structures of the turbulent flow.

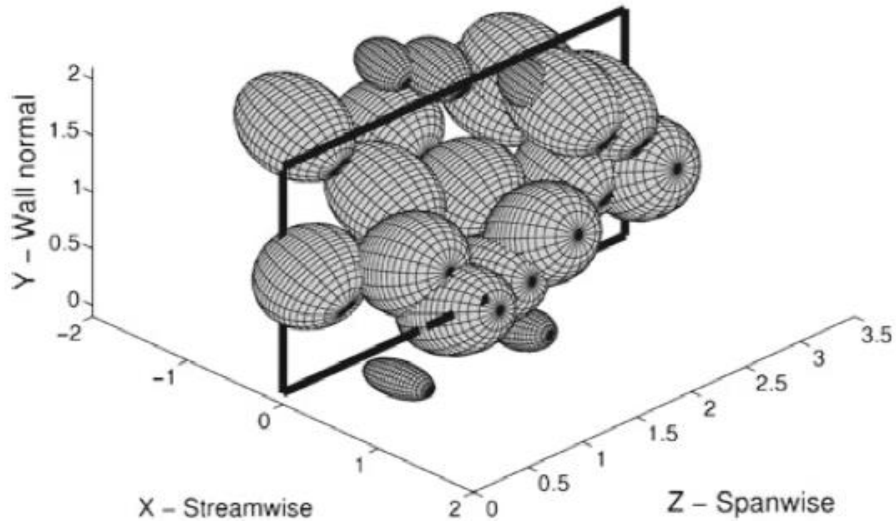


(from Poletto *et al. FTC, 2013)*

**References**

**SEM Basic form:** (Jarrin *et al.*, *Int. J. Heat Fluid Fl.*, 2006), (Jarrin, *PhD of the University of Manchester*, 2008), (Jarrin *et al.*, *Int. J. Heat Fluid Fl.*, 2009)
**SEM for wall-bounded flows:** (Pamiès *et al.*, *Phys. Fluids, 2009)*
**Divergence free SEM** *(*Poletto *et al.*, *Flow, Turbulence and Combustion*, 2013*)*

# Experiment – simulation: example of connection to develop unsteady inlet BC for DNS with the SEM (inlet of MAVERIC rig)

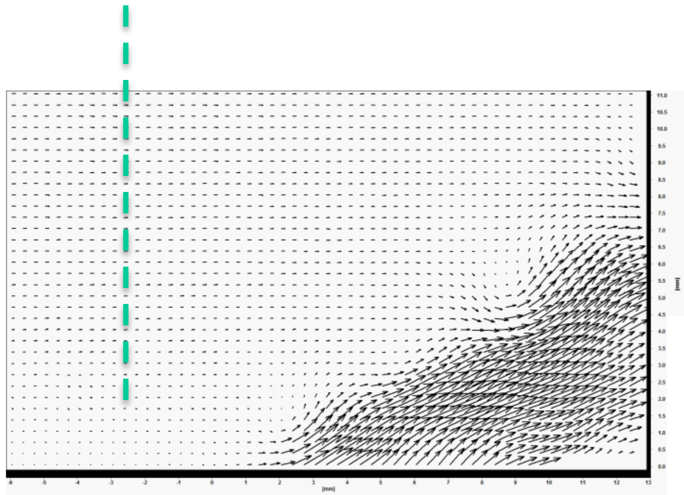

Measurements: provide some of the targeted values for the SEM

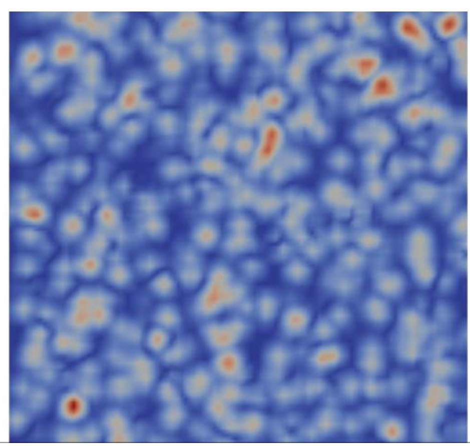

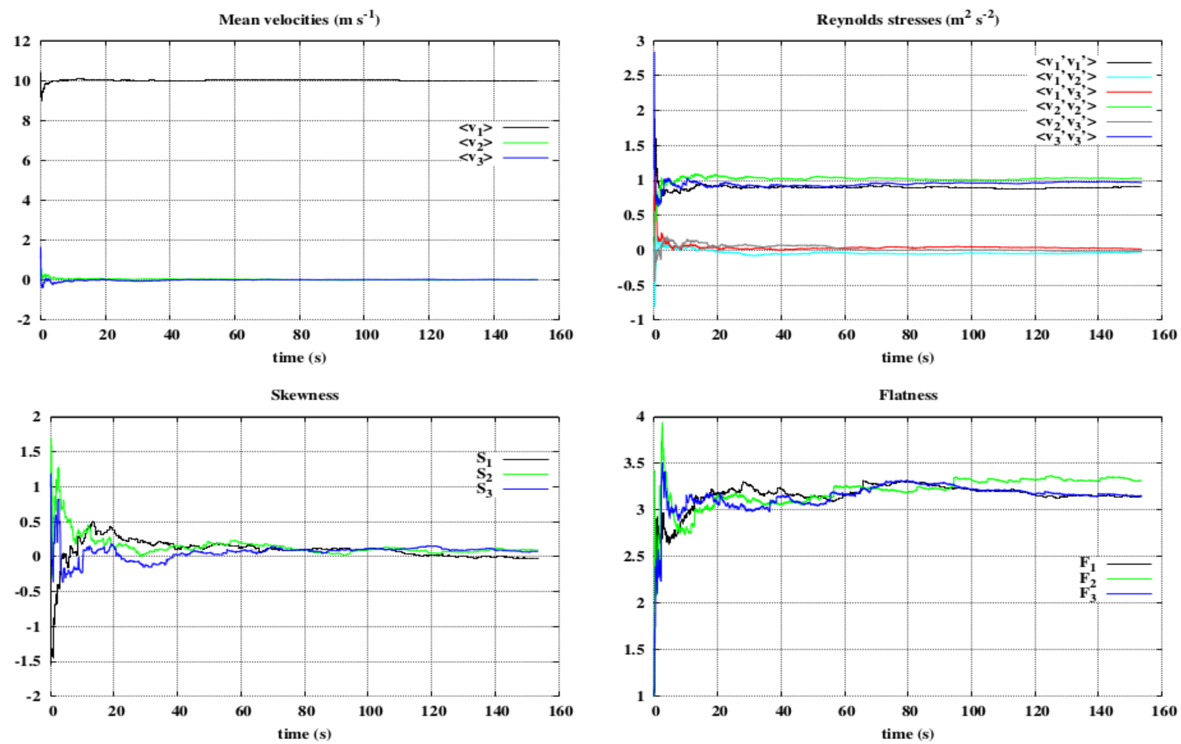

## Incoprorating a STG approach into a compressible Euler solver: the ATCBC method at a subsonic inlet (Moguen et al., 2014)

Consider a one-dimensional flow governed by the Euler equation for simplicity, thus the temporal rates of change of the wave amplitudes are given by:

$$L_1 = (v-c)\left(\frac{1}{\rho c}\partial_x p - \partial_x v\right) \quad \text{upstream travelling acoustic wave}$$

$$L_2 = v\,\left(\partial_x \rho - \frac{1}{c^2}\partial_x p\right) \quad \text{entropy wave}$$

$$L_3 = (v+c)\left(\frac{1}{\rho c}\partial_x p + \partial_x v\right) \quad \text{downstream travelling acoustic wave}$$

## Incoprorating a STG approach into a compressible Euler solver: the ATCBC method at a subsonic inlet

These *Li*'s satisfy the following LODI system at the inlet:

$$\partial_t \rho + \frac{\rho}{2c}(L_1 + L_3) + L_2 = 0 \quad (1a)$$

$$\partial_t v + \frac{1}{2}(L_3 - L_1) = 0 \quad (1b)$$

$$\partial_t p + \frac{\rho c}{2}(L_1 + L_3) = 0 \quad (1c)$$

**Subsonic inlet (1D):** Two Li's have to be imposed.

**Main hypothesis** (**H1**) **behind the ATCBC method to avoid reflection**: at the inlet, the gap (if any) between the targeted velocity $v^{\dagger}$ coming from the STG process and the current one v is solely attributed to the upstream travelling acoustic wave.

**Methodology to check the proposal coherence at low Mach**: two-scale asymptotic analysis of the LODI system.

## Incoprorating a STG approach into a compressible solver: the ATCBC method at a subsonic inlet

From (1b), **H1** is enforced by assuming that:

$$\partial_t (v - v^\dagger) + \frac{1}{2}(0 - L_1) = 0$$

which is achieved by imposing that: $-2\,\partial_t v^\dagger = L_3$

The remaining boundary condition is derived by 1) assuming a frozen turbulence hypothesis (**H2**) and 2) asymptotically expanding $L_2$ which finally yields $L_2 = 0$ (at order -1 and 0).

# Example of different tests when setting-up the ATCBC method

Harmonic inlet signal

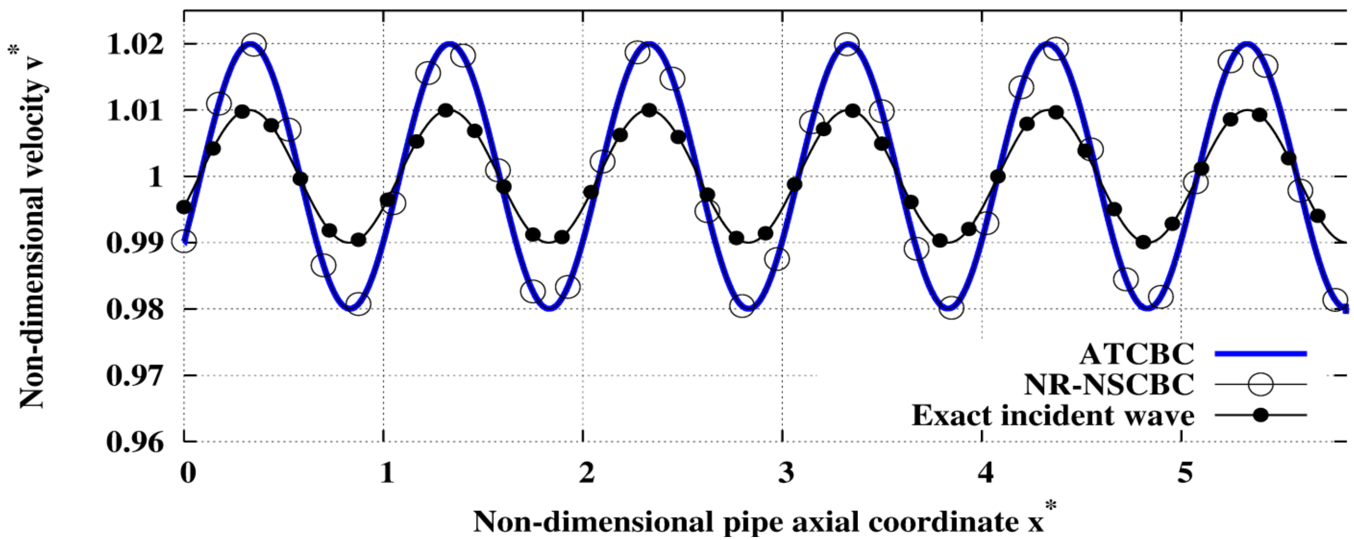


Harmonic inlet signal + a STG signal (Non linear Langevin equation)

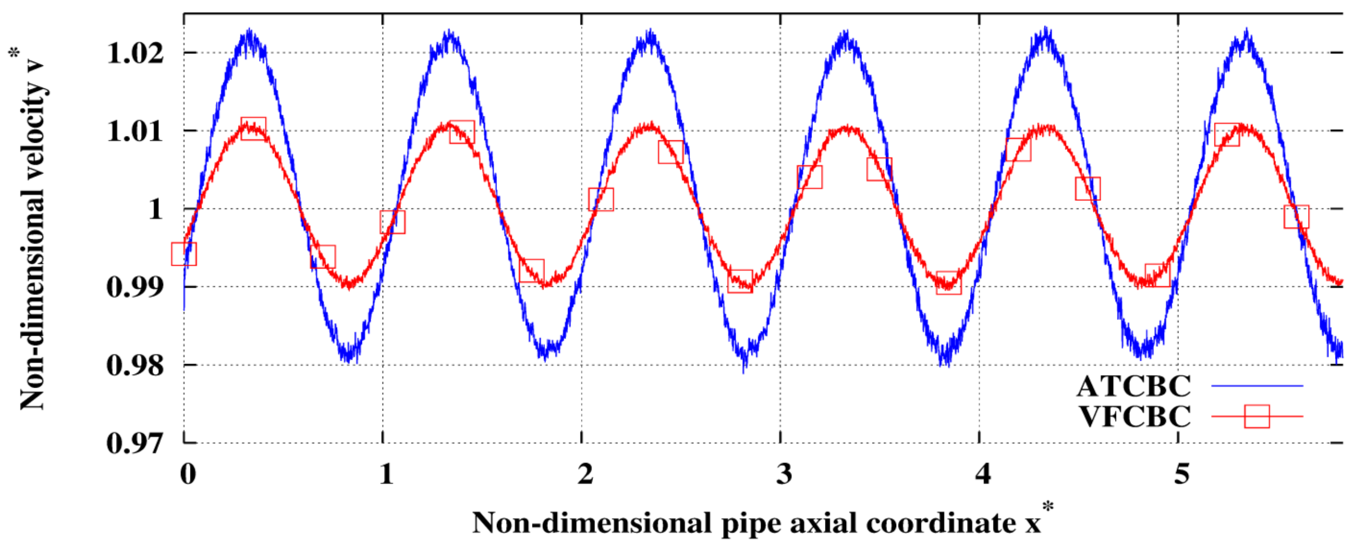

# Recent Cagire references related to low/all Mach number flow simulation issues


1. Dellacherie, S., Jung, J., Omnes, P., Raviart, P.-A. (2016) *Construction of modified Godunov type schemes accurate at any Mach number for the compressible Euler system*, Mathematical Models and Methods in Applied Sciences, Vol. 26, No. 13, pp. 2525–2615.

2. Dellacherie, S., Jung, J., Omnes, P. (2016), *Preliminary results for the study of the Godunov scheme applied to the linear wave equation with porosity at low Mach number*, ESAIM: Proceedings and Surveys, Vol. 52, pp. 105-126.

3. Delmas, S. (2015) « *Simulation numérique directe d'un jet en écoulement transverse à bas nombre de Mach en vue de l'amélioration du refroidissement par effusion des chambres de combustion aéronautiques* », PhD thesis, Pau and Pays de l'Adour University, France.

4. Moguen, Y., Bruel, P., Dick, E. (2015a) "*Solving low Mach number Riemann problems by a momentum interpolation method*", Journal of Computational Physics, Vol. 298, pp. 741-746.

5. Moguen, Y, Delmas, S., Perrier, V., Bruel, P., Dick, E. (2015b) "*Godunov-type schemes with inertia terms for unsteady full Mach number range flow calculations*", Journal of Computational Physics, Vol. 281, pp. 556-590.

# Recent Cagire references related to low/all Mach number flow simulation issues


6. Moguen, Y., Bruel, P., Perrier, V., Dick, E. (2014) “*Non-reflective inlet conditions for the calculation of unsteady turbulent compressible flows at low Mach number”,* Mechanics and Industry, Vol. 15, No 3, pp. 179-189.

7. Moguen, Y**.,** Bruel, P., Dick, E. (2013) “*Semi-implicit characteristic-based boundary treatment for acoustics in low Mach number flows*”, Journal of Computational Physics, Vol. 255, pp. 339-361.
8. Moguen, Y., Dick, E., Vierendeels, J., Bruel, P. (2013) “*Pressure-velocity coupling for unsteady low Mach number flow simulations: an improvement of the AUSM+-up scheme”,* Journal of Computational and Applied Mathematics, Vol. 246, pp. 136-143.

9. Moguen, Y., Kousksou, T., Bruel, P., Vierendeels, J. and Dick, E. (2012) “*Pressure-velocity coupling allowing acoustic calculation in low Mach number flow*”, Journal of Computational Physics, Vol. 231, pp. 5522-5541.